FINAL REPORT

to

NASA-AMES UNIVERSITY CONSORTIUM

NASA-AMES RESEARCH CENTER

on

INORGANIC WATER REPELLENT COATINGS FOR THERMAL PROTECTION INSULATION ON AN AEROSPACE VEHICLE

Grant No. NCC2-5139

prepared by

D. W. Fuerstenau, Principal Investigator
P. Huang
R. Ravikumar

Department of Materials Science and Mineral Engineeing
University of California
Berkeley, CA 74720-1760

November 1997

ABSTRACT

The objective of this research was two-fold: first, to identify and test inorganic water-repellent materials that would be hydrophobic even after thermal cycling to temperatures above 600 °C and, second, to develop a model that would link hydrophobicity of a material to the chemical properties of its constituent atoms. Four different materials were selected for detailed experimental study, namely, boron nitride, talc, molybdenite, and pyrophyllite, all of which have a layered structure made up of ionic/covalent bonds within the layers but with van der Waals bonds between the layers. The materials tested could be considered hydrophobic for a nonporous surface but none of the observed contact angles exceeded the necessary 90 degrees required for water repellency of porous materials. Boron nitride and talc were observed to retain their water-repellency when heated in air to temperatures that did not exceed 800 °C, and molybdenite was found to be retain its hydrophobicity when heated to temperatures up to 600 °C. For these three materials, oxidation and decomposition were identified to be the main cause for the breakdown of water repellency after repeated thermal cycling. Pyrophyllite shows the maximum promise as a potential water-repellent inorganic material, which, when treated initially at 900 °C, retained its shape and remained hydrophobic for two thermal cycles where the maximum retreatment temperature is 900 °C. A model was developed for predicting materials that might exhibit hydrophobicity by linking two chemical properties, namely, that the constituent ions of the compound belong to the soft acid-base category and that the fractional ionic character of the bonds be less than about 20 percent.

I. INTRODUCTION

Thermal protection systems (TPS) for a reusable space launch vehicle are expected to be a maturation of developed technology. These materials are similar to those used on the Shuttle. Two materials which are TPS candidates are blankets and tiles, whose major components are silica and alumina [1, 2, 3]. As fabricated, these materials are hydrophilic and without protection can imbibe water [4]. Since this water results not only in a weight penalty but also, under certain conditions, damage to the TPS, the TPS must be waterproofed [4]. The procedure used today for waterproofing the Shuttle is not permanent [4, 5]. The waterproofing agents, silane derivatives, though extremely effective for waterproof-ing, create a hydrophobic coating which decomposes at the high temperatures experienced by the TPS during reentry [4, 5]. This requires the TPS to be rewaterproofed after every flight. Although attempts have been made to extend the silane agents usefulness to higher tempera-tures, these have proved to be unsuccessful. Agents that are of organic nature are inherently limited at high temperatures in an oxidative environment [6, 7].

A prime driver in the new launch vehicle design is operational efficiency. A permanent waterproofed TPS which retains its hydrophobicity after thermal cycling such as repeated reentries, would enhance the efficiency, minimizing operation, by reducing maintenance time and cost. A permanent waterproofing process to date has remained elusive. One reason is that most waterproofing is required for materials at moderate temperatures and therefore organic-based agents can be used. Inorganic agents which may have greater stability, have generally been used as water barriers or membranes but rarely as water-repellent coating. A suitable water-repellent film would have to be deposited on the TPS by surface-coating techniques [8].

Water-repellent inorganics exist, though few occur naturally. Three hydrophobic minerals are talc, stibnite, and molybdenite. Their hydrophobicity is of importance in mineral processing and the relationship between hydrophobicity and their properties has been studied [9]. However, factors that control the hydrophobicity or water repellency of inorganic

materials have never been fully investigated as of yet. A proper understanding of these factors might lead to the development of new inorganic coating materials which will remain hydrophobic after thermal cycling.

The objective of the research reported here was to investigate and define factors that control the hydrophobicity of inorganic materials, including the development of a model for characterizing the hydrophobicity of such materials. Most of the published investigations conducted on the principles of hydrophobicity have been concerned with the behavior of organic polymers, but our efforts required the extension of concepts to and the determination of factors that lead to water repellency in inorganic materials. After model development, the hydrophobicity of selected materials was studied experimentally to verify the model. In particular, the effect of thermal cycling on the hydrophobicity and chemical stability of these materials was investigated.

II. REVIEW OF WETTABILITY PHENOMENA

When a small amount of liquid is placed on a solid surface, it may spread on the surface to form a film or it may retract from the surface into beads. The affinity of the solid for the liquid is referred to as its wettability. On a molecular scale, the interactions between molecules that contribute to wettability may be due to long-range London-van der Waals forces (often now called Lifshitz-van der Waals), electrical effects, and acid-base (hydrogen bonding) interactions. In the case of aqueous systems, the hydrophobicity of a material arises because of its non-interaction with water molecules. Hydrophobicity results from the water molecules having greater attraction for themselves than for the solid substrate.

Detailed presentations of various aspects of wettability phenomena discussed here can be obtained from a number of sources [10-14]. In this section, the most important relationships that control the wettability of materials and their water repellency are briefly reviewed.

Contact Angles and Equilibrium in Partially-Wetted System

For three-phase solid/liquid/vapor systems that partially wet, the three phases are in contact along a line. A quantitative measure of the wetting of a solid by a liquid is the contact angle, which is the angle perpendicular to the line of the contact, measured across the liquid phase. If a solid surface is fully wet by the liquid, the contact angle is zero.

Equilibrium in these systems is controlled by the balance of surface tensions or surface free energies at the three interfaces: solid/liquid (SL), solid/vapor (SV), and liquid/vapor (LV). In a partially-wet system where the contact angle is finite, equilibrium is given by the Young equation (which can be derived either by a balance of forces on the sessile drop shown in Figure 1 or from surface free energy minimization):

$$\gamma_{SV} - \gamma_{SL} - \gamma_{LV} \cos\theta = 0 \qquad (1)$$

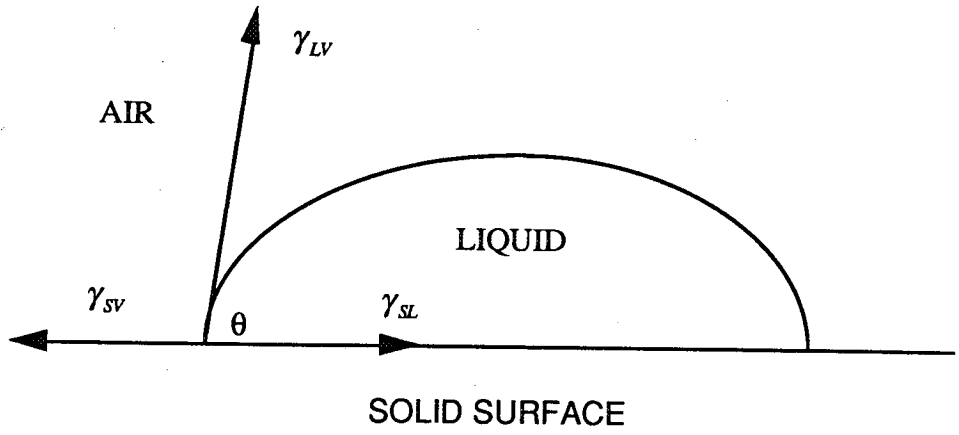

Figure 1- Schematic representation of a sessile drop of water on a flat surface, showing the contact angle measured through the liquid phase and the interfacial tensions at the three interfaces (SV, SL and LV).

where θ is the contact angle and γ is the surface tension (or surface free energy per unit area) and subscripts SV, SL, and LV refer to the solid-vapor, solid-liquid, and liquid-vapor interface, respectively.

Eq. 1 is valid only for finite values of the contact angle. As already stated, when a liquid completely wets a surface, the contact angle is zero so a spreading coefficient, $S_{S/L}$, is used to relate the forces involved:

$$S_{L/S} = \gamma_{SV} - \gamma_{LV} - \gamma_{SL} \qquad (2)$$

When the term $S_{L/S}$ is positive, then the spreading of a liquid on a solid surface is spontaneous.

Thermodynamically, the surface or interfacial tension is defined as the change in the Gibbs surface free energy with the change in surface area, A, at constant T, P and adsorption of the various components in the system:

$$\gamma_{LV} = \left(\frac{\partial G_{LV}}{\partial A_{LV}}\right)_{T,P,ads.equilib.} \qquad (3)$$

Gibbs [10] derived a relation that relates the effect of adsorption on the surface tension:

$$d\gamma = -RT\Gamma_i d\ln a_i \tag{4}$$

where Γ_i is the adsorption density of species *i* at a interface and a_i is its activity in solution or in the gas phase.

Since adsorption of vapor might occur at the solid-vapor interface, the Young equation is often written in the form

$$\gamma_S - \pi_e - \gamma_{SL} - \gamma_{LV}\cos\theta = 0 \tag{5}$$

where γ_S is the surface tension of solid in vacuum and π_e is the reduction in surface tension resulting from the adsorption of vapor (water) molecules at the solid/gas interface. Generally, the liquid/vapor and liquid/vacuum surface tensions are essentially identical. For ambient-temperature applications, water repellency can be achieved through the adsorption of organic surfactants that regulate surface tensions in accordance with Eq. 4.

Work of Adhesion

The work of adhesion, W_A, is defined as the work required to separate unit area of solid/liquid interface to produce a solid/vacuum and a liquid/vacuum interface.

$$W_A = \gamma_S + \gamma_L - \gamma_{SL} \tag{6}$$

W_A is equivalent to the negative free energy change associated with contacting a solid with the liquid, or adhesion of the two phases:

$$W_A = -\Delta G_{adhesion} \tag{7}$$

Substitution of the Young equation into the equation defining the work of adhesion yields:

$$W_A = \gamma_{LV}(1 + \cos\theta) \tag{8}$$

This equation is valid for systems where adsorption at the solid/vapor or liquid/vapor interface is absent. If adsorption at the solid/vapor interface does occur, then the work of adhesion is given by

$$W_A = \gamma_{LV} (1 + \cos\theta) + \pi_e \qquad (9)$$

The common definition of work of adhesion (Eq. 6) certainly defines a nonequilibrium process. In fact, Johnson and Dettre [11] define Eq. 6 as a "nonequilibrium" work of adhesion and define the "equilibrium" work of adhesion in terms of creating a solid/vapor interface rather than a solid/vacuum interface.

Molecular interactions are often expressed in terms of the work of cohesion, W_C, which is defined (in the case of a liquid) as the work required for separating a column of liquid into two parts, creating two liquid/vapor interfaces:

$$W_C = 2\gamma_{LV} \qquad (10)$$

From Eq. 8 and 10, a useful equation relating the competition between adhesive forces, W_A, and cohesive forces, W_C, follows:

$$\cos\theta = 2\frac{W_A}{W_C} - 1 \qquad (11)$$

The Wetting of Materials

Nonporous Materials

Some wetting processes involve the spreading of a liquid over a flat surface. Here the work of spreading, W_S, is defined as the work required to expose unit area of solid/vacuum interface while destroying a corresponding amount of solid/liquid and liquid/vapor interface:

$$W_S = \gamma_S - \gamma_L - \gamma_{SL} \qquad (2a)$$

Spreading is controlled by Eq. 2 and not by the defined relation given by Eq. 2a. If adsorption occurs, Eq. 2a should also be modified with the π_e term, making it identical to Eq. 2. With the Young equation,

$$W_s = \gamma_{LV} (\cos\theta - 1) \tag{12}$$

Positive spreading occurs only when $\theta = 0°$. For any flat system in the absence of gravitational effects, dewetting should occur whenever there is a finite contact angle.

Porous Materials

In the case of porous materials, wetting processes involve the displacement of the vapor phase within a pore by a liquid. In these systems, dewetting involves the creation of a solid/vacuum (actually solid/vapor) interface and the destruction of a solid/liquid interface. In the analog of a pore as being a capillary, the liquid/vapor interfacial area remains constant. For wetting in such a system, the free energy for capillary wetting, ΔG_{cap}, is defined as the free energy change to produce unit area of solid/liquid interface while destroying unit area of solid/vapor interface:

$$\Delta G_{cap} = \gamma_{SL} - \gamma_{SV} \tag{13}$$

or with the Young equation:

$$\Delta G_{cap} = -\gamma_{LV} \cos\theta \tag{14}$$

Thus, water will penetrate the capillary pores whenever the contact angle is less than 90 degrees. *This means that the contact angle criterion for water repellency with porous materials requires that the contact angle should be at least 90 degrees.*

The penetration of liquid and the wetting behavior of porous materials results from the fact that the pressure under a curved interface is less than that under a flat surface, the pressure difference ΔP being given by the following relation:

$$\Delta P = 2\gamma/r \tag{15}$$

where r is the radius of curvature. If there is a contact angle, then the pressure difference over the liquid in a capillary of radius r is

$$\Delta P = \frac{2\gamma \cos\theta}{r} \tag{15a}$$

This pressure difference across the interface leads to the Kelvin equation, which quantifies the reduction in vapor pressure over a concave surface. These phenomena lead to capillary condensation in porous media when the contact angle is less than 90 degrees [10]. If the contact angle is 90 degrees, there is no pressure difference across the interface.

Heterogeneous Surfaces

If two different phases make up a solid or if the solid particle exhibits highly anisotropic crystallinity, the material can be considered to have a composite surface made up of types of patches. As considered by Cassie [10, 11], if the fraction of component 1 in the surface is f_1 and that of component 2 in the surface is f_2 where θ_1 is the contact angle of material 1 and θ_2 that of material 2, the apparent contact angle of the composite surface, θ_c, is given by

$$\cos\theta_c = f_1 \cos\theta_1 + f_2 \cos\theta_2 \tag{16}$$

For the case of a porous solid, where fraction 2 is air, the Cassie relation is modified as :

$$\cos\theta_c = f_1 \cos\theta_1 - f_2 \tag{17}$$

Therefore, for porous solids, the apparent contact angles are slightly higher.

In the case of a solid with a rough surface, the apparent contact angles may also differ from those on smooth surfaces, depending on the degree of roughness and the magnitude of

the contact angle [10]. For a rough solid where the coefficient, R, is the ratio of the actual surface area to the apparent or the projected area, the relation between them is

$$\cos\theta_R = R\cos\theta_I \tag{18}$$

When the contact angle is less than 90 degrees, roughness tends to decrease its apparent magnitude and when the angles are greater than 90 degrees, the apparent contact angle is increased. Nonhomogeneity and roughness tend to cause hysteresis in contact angle measurements, that is differences between measured liquid-advancing and liquid-receding contact angles are observed.

Measurement of Contact Angles

Various methods exist for the measurement of the contact angle of a liquid on a solid surface [10, 15]. Some of these methods involve the direct measurement of the angle whereas others are based on indirect force determinations. Quite commonly, contact angles are measured directly by the captive-bubble method or by the sessile drop method. In our studies, we have used the sessile drop method. Here, a drop of liquid, water in this case, is placed on the solid surface and the contact angle is measured through a goniometer. This angle is sometimes reported as the advancing contact angle. When the water is removed from the surface by some method, the angle measured between the water and the solid surface corresponds to the receding contact angle. For some of their work, Zisman and coworkers [15] simply continued to add water to the sessile drop until it reached the equilibrium Quincke height, which is determined by the surface tension and the density of the liquid and the contact angle. For a pure liquid, their only measurement was the height of large drop of liquid. Another direct measurement was Adam's tilting plate method wherein a flat plate was tilted to the angle at which the liquid surface remained flat right up to the solid. The Wilhelmy slide plate method involves weighing a thin plate partially immersed in a liquid. The measured weight includes the weight of the plate and the vertical component of the surface tension acting

on the plate perimeter. Neumann developed an accurate Wilhelmy slide technique that involved measuring the height of the meniscus on a vertical plate partially immersed in the liquid, the height being controlled by the surface tension of the liquid, its density and the contact angle. For finely divided solids, the capillary force method can be used by preparing a compacted plug of the particles. Here, the material is considered like a bunch of capillaries and the pressure required to push or remove the fluid from the pores is measured. The Laplace equation (Eq. 15a) relates the contact angle to the liquid surface tension and the radius of the pores. The radius r is determined by measuring the pressure required to prevent a wetting liquid from entering the pores (Eq. 15). Fuerstenau et al. [16] have presented a method for determining the contact angles by measuring the mean critical wetting surface tension of the particles by film flotation and quantifying the results in combination with the Neumann-Good equation of state.

The Hydrophobicity of Materials

Molecular Interactions and Hydrophobicity

The most basic factor in wetting in a solid/liquid/gas system is the free energy of interaction between the liquid and solid phases across the interface. This free energy of interaction is equal numerically, but of opposite sign, to the reversible work of adhesion. Fowkes [13] was the first to clearly separate the various contributions to interactions across the solid/liquid interface to include not only London-Lifshitz-van der Waals dispersion forces but also other polar interactions and the electrostatic attraction/repulsion of electrical double layers. He considered the work of adhesion, W_A, to be the sum of these various interactions. In a classic paper on factors that control the wettability of silica, Laskowski and Kitchener [17] interpreted the work of adhesion by analyzing it with respect to the relative magnitude of three main terms: the dispersion forces, the hydration of nonionic polar sites, and surface ionization. Their expression for the work of adhesion for water to a solid is

$$W_A = W_A^d + W_A^h + W_A^{el} \qquad (19)$$

where W^d is the contribution from dispersion forces (London-Lifshitz-van der Waals), W^h represents contributions due to the hydrogen bonding of water with surface hydroxyl sites, and W^{el} estimates the contribution from ionic sites on the surface (the electrical double layer). Usually a solid is hydrophobic when the contributions from the electrical and hydrogen bonding terms are small. Citing data for a wide range of materials, Laskowski and Kitchener [17] showed that, because of the exceptionally large value of the work of cohesion of water, the work of adhesion is always less than the work of cohesion of water and concluded that, "*all solids would be hydrophobic if they did not carry polar or ionic groups.*"

Subsquently, Fowkes [11, 18] expressed the polar interactions at the solid/liquid interfaces in terms of acid-base phenomena so that the work of adhesion to be written as

$$W_A = W_A^d + W_A^{AB} + W_A^{el} \tag{20}$$

where W_A^{AB} represents acid-base interactions (such as Lewis acid-Lewis base) between surface sites and liquid molecules. The silanation procedure currently being used to waterproof the silica/alumina TPS on the Shuttle functions by covering up the polar sites that would otherwise hydrogen bond with water molecules.

Ideal Nonpolar Surfaces

When water molecules are near completely nonpolar surfaces, the hydrogen bonding and electrical interaction terms between water molecules and the solid surface become negligible and only the dispersion forces due to London-Lifshitz-van der Waals forces dominate. Under these conditions, Fowkes [19] proposed a way to estimate the interfacial energy between a solid and a liquid using the following expression:

$$\gamma_{SL} = \gamma_S + \gamma_L - 2\sqrt{\gamma_S^d \gamma_L^d} \tag{21}$$

Interaction across such interfaces is only through dispersion forces, so the interfacial tension between the two phases is the surface tension of the liquid plus that of the solid minus twice the geometric mean of the dispersion force interactions.

When interaction is only due to dispersion forces, Eq. 11 can be modified as

$$\cos\theta = \frac{2W_A^d}{W_C} - 1 \tag{22}$$

which gives

$$\cos\theta = -1 + 2\sqrt{\gamma_S^d}\left(\frac{\sqrt{\gamma_L^d}}{\gamma_L}\right) \tag{23}$$

Eq. 23 is sometime called the Girifalco-Good-Fowkes-Young equation. For a series of liquids of different surface tensions, a plot of $\cos\theta$ versus $\sqrt{\gamma_L^d}/\gamma_L$ gives a straight line of slope $2\sqrt{\gamma_s^d}$. Using a series of hydrocarbons where $\gamma_L = \gamma_L^d$, Fowkes determined the value of dispersion forces in liquid water to be $\gamma_w^d = 22$ ergs/cm^2, and for most saturated hydrocarbons, the value of the their surface tension is essentially the value of its dispersion component.

Hydrophobic Materials

Probably the most comprehensive paper dealing with the hydrophobicity of natural materials was that of Gaudin et al. [20], who related flotation response to crystal structure. Most of the researchers in flotation believed that hydrocarbon groups of adsorbed surfactants were required for imparting flotability to minerals. Laskowski and Kitchener's work [17] clearly showed that the role of adsorbed organic coatings in imparting hydrophobicity is to cover up the polar sites on the surface, thereby preventing hydration. Gaudin et al. showed that *native floatability* (that is, possession of inherent water repellency without the addition of an organic surfactant) *results when at least some fracture or cleavage surfaces form without rupture of interatomic bonds other than residual bonds*. They further showed that the natural

lack of floatability results when all natural fracture or cleavage surfaces offer ionic bonds to the surrounding aqueous phase in greater density than some threshold value. In effect, Gaudin's concepts were that crystals held together by residual van der Waals bonds would provide a nonpolar surface and hence be floatable without the addition of a surfactant. One kind of example of such materials are molecular crystals which are made up of finite molecules, such as sulfur (S_8) or paraffin wax ($C_{30}H_{62}$), held together in the crystal by van der Waals forces. Such materials do not exhibit anisotropy in their surface characteristics.

Other crystals consist of infinite two-dimensional sheet structures, with the sheets held together by van der Waals forces. However, within the sheets the atoms are held together by covalent bonds as with graphite or by hydrogen bonds for boric acid [$B(OH)_3$] or ionic/covalent bonds in the case of complex silicate mineral talc. Wetting anisotropy in such crystals can result. Cleavage between the sheets gives rise to nonpolar surfaces where acid-base and electrical interactions are absent, but the fracture of the crystal that forms edges results from broken primary bonds so that interactions on edges include van der Waals plus acid-base plus electrical effects [20, 21, 22]. Thus such crystals may have hydrophobic faces but hydrophilic edges.

Adamson [10] has tabulated published data on the contact angles of selected materials, and examples for water are given in Table 1. Crystals of all of those materials given in this table are held together by residual van der Waals bonds, except for silver iodide (ionic/covalent bonding) and platinum (metallic bonding). The materials considered in this project were inorganic materials that should (or might) exhibit not only hydrophobicity but also high-temperature stabiliity.

Table 1 -Selected contact angle data for various materials in water/air systems at 20-25°C (after Adamson [10]).

Material	Contact Angle, degrees
Paraffin	110
PTFE (Tefllon)	112
Polyethylene	103
Stibnite (Sb_2S_3)	84
Graphite	86
Sulfur	78
Pyrolytic carbon	72
Platinum	40
Silver iodide	17
Gold*	0

* There as been controversy over the existence of a contact angle on gold [19]. Since clean mercury has a maximum contact angle of about 103 degrees, one might expect one on gold also. Surface oxidation may give rise to surface hydration sites on gold.

III. POTENTIAL CANDIDATE MATERIALS

In this section, we will tabulate some of the compounds that might potentially be used as an inorganic high-temperature water-repellent material. Also, some of the properties of the naturally occurring room-temperature materials will be summarized.

Most naturally occurring hydrophobic materials have layered structures that are held together by weak van der Waals forces between them. In the search for potential inorganic water-repellent materials, a list of compounds was first compiled, most of them possessing a layered structure. The inorganic water-repellent compound might eventually become a coating on the thermal protection system materials (alumina and silica) of the space shuttle. Since, during re-entry, the shuttle experiences surface temperatures in the range of 1000 °C, it is important to know the transformation properties of the inorganic materials in the compiled list. Therefore, in Tables 2a - 2l we have listed some of the inorganic compounds considered for our study in terms of their crystal structure or geometry of packing and their melting temperatures. Here in these tables, we have also classified the various materials into different categories, according to their chemical forms, elements and compounds (where they are further sub-divided according to their anionic functional group, namely halides, sulfides, oxides, carbides, selenides, tellurides and diborides). The sources of the data summarized in these tables were Physical Constants of Inorganic Compounds, CRC Handbook of Chemistry and Physics [23] and Handbook of Refractory Compounds [24]. Wells [43] has given a thorough discussion of structural inorganic chemistry, such as that for cadmium iodide and chloride.

For the naturally occurring hydrophobic materials, the most common forms of breakdown of water repellency at high temperature corresponds to one of the following mechanisms:

1. Phase transformation: Here the material may change its physical state from solid to liquid or sublime to a gas; or it might recrystallize as a solid having another crystal structure.

2. Oxidation: In air at high temperature, the material may undergo oxidation, either at the surface or completely if the material is highly reactive. The corresponding oxide form may interact with water, thereby rendering the material hydrophobic.
3. Decomposition: This mechanism is particular to the two-layered complex oxide material, such as talc and pyrophyllite, where upon heating they undergo dehydroxylation.

Most of the naturally occurring hydrophobic inorganic materials belong to the class of layered compounds, as exemplified by graphite, talc, pyrophyllite, and molybdenite. Others belong to the class of molecular crystals or chain-type compounds. In the various compounds that exhibit hydrophobicity, the main force linking the layers or the chains or the molecular to form crystals is generally van der Waals interaction. Within the layer or chain or molecular crystal arrangements, either covalent or ionic bonding may exist. Some of the mechanisms of breakdown of hydrophobicity of naturally occurring water-repellent materials is also listed in Table 3, along with the contact angles which they exhibit with water at room temperature.

Surface oxidation phenomena plays an important role in the hydrophobicity of materials, such as sulfide minerals. M. C. Fuerstenau and Sabacky [25] found that when sulfide minerals are comminuted under conditions in which oxygen is totally absent and subjected to flotation in water containing only 5 ppb of oxygen, all sulfide minerals are naturally flotable. In the presence of oxygen, however, they become hydrophilic. Chander and Fuerstenau [26] have noted that molybdenite is not only readily naturally hydrophobic because of its crystal chemistry, but it retains its hydrophobicity in the presence of oxidizing conditions because the oxidation products are soluble anions (molybdate ions). In the case of Cu, Fe, Pb and Zn sulfides, in contrast, the soluble cations hydrolyze to insoluble hydrous hydroxides that adsorb on the sulfide, causing the sulfide mineral to become strongly hydrophilic.

Table 2(a) - Potential materials for inorganic water repellents

Category: ELEMENTS

Material Name	Chemical Formula	Crystal Structure	Melting Point (°C)
Gold	Au	fcc*, 3-D	1064.3
Diamond	C	dc*, 3-D	3827
Graphite	C	hcp*, Layer	3627
Selenium	Se	Chain	217
Arsenic	As	Layer	817
Antimony	Sb	Layer	630.76
Bismuth	Bi	Layer	1564
Phosphorus	P	Layer	NA*
Sulfur	S_8	Chain	112.8

* fcc = face centered cubic, hcp = hexagonal close-packing, dc = diamond cubic, NA = not available

Table 2(b) - Potential materials for inorganic water repellents

Category: (HALIDES) BROMIDES

Material Name	Chemical Formula	Crystal Structure	Melting Point (°C)
Silver bromide (Bromyrite)	AgBr	NaCl/fcc, 3-D	432
Cadmium bromide	$CdBr_2$	CdI_2 / hcp, Layer	567
Cobalt bromide	$CoBr_2$	$CdBr_2$	678 (in N_2)
Iron bromide	$FeBr_2$	$CdBr_2$	684 (?)
Nickel bromide	$NiBr_2$	$CdBr_2$	963
Magnesium bromide	$MgBr_2$	$CdBr_2$	700
Manganese bromide	$MnBr_2$	$CdBr_2$	d.* (at room temp.)
Titanium bromide	$TiBr_2$	$CdBr_2$	d>500
Vanadium bromide	VBr_2	$CdBr_2$	d. (at room temp.)
Zinc bromide	$ZnBr_2$	$CdCl_2$ / hcp, Layer	394

* d = decomposes

Table 2(c) - Potential materials for inorganic water repellents

Category: (HALIDES) CHLORIDES

Material Name	Chemical Formula	Crystal Structure	Melting Point ° C
Silver chloride (Chlorargrite)	AgCl	NaCl / fcc, 3-D	455
Cadmium chloride	$CdCl_2$	ccp*, Layer	568
Cobalt chloride	$CoCl_2$	$CdCl_2$	724 (in HCl)
Nickel chloride	$NiCl_2$	$CdCl_2$	1009
Magnesium chloride	$MgCl_2$	$CdCl_2$	714
Vanadium chloride	VCl_2	CdI_2	1350

* ccp = cubic close-packing

Table 2(d) - Potential materials for inorganic water repellents

Category: (HALIDES) IODIDES

Material Name	Chemical Formula	Crystal Structure	Melting Point (°C)
Silver iodide (Iodyrite)	AgI	Wurtzite, 3-D	558
Cesium iodide	CsI	CsCl / bcc*	626
Germanium iodide	GeI	CdI_2	d. (at room temp.)
Cadmium iodide	CdI_2	hcp, Layer	387
Calcium iodide	CaI_2	CdI_2	784
Cobalt iodide	CoI_2	CdI_2	515 (Vac.*)
Iron iodide	FeI_2	CdI_2	Red Heat
Magnesium iodide	MgI_2	CdI_2	<637
Manganese iodide	MnI_2	CdI_2	d<637
Lead iodide	PbI_2	CdI_2	402 (Pois.*)
Thorium iodide	ThI_2	CdI_2	a 650, b 864
Titanium iodide	TiI_2	CdI_2	600
Yttrium iodide	YI_2	CdI_2	NA
Zinc iodide	ZnI_2	CdI_2	446

* bcc = body centered cubic, Vac = Vacuum, Pois = Poisonous

Table 2(e) - Potential materials for inorganic water repellents

Category: OXIDES

Material Name	Chemical Formula	Crystal Structure	Melting Point (°C)
Claudetite	As_2O_3	Monoclinic, Layer	193 (subl. 312.3)
Arsenic oxide	As_4O_6	Molecular crystal	193 (subl. 312.3)
Chromium oxide	CrO_3	Chain	196
Boric Acid	H_3BO_3	Layer	169
Mercuric oxide	HgO	hcp / orthorhombic Layer / 3-D	500 (d)
Molybdenum oxide	MoO_3	Layer	795
Lead oxide	PbO	Tetragonal, Layer	886
Antimony oxide (Valentinite)	Sb_2O_3	Orthorhombic double chain	656
Selenium oxide	SeO_2	Chain	340-350

Table 2(f) - Potential materials for inorganic water repellents

Category: COMPLEX OXIDES

Material Name	Chemical Formula	Crystal Structure	Melting Point (°C)
Pyrophyllite	$Al_2(Si_4O_{10})(OH)_2$	Monoclinic, Layer	
Talc	$Mg_3(Si_4O_{10})(OH)_2$	Monoclinic, Layer	850 (d)

Table 2(g) - Potential materials for inorganic water repellents

Category: SELENIDES

Material Name	Chemical Formula	Crystal Structure	Melting Point (°C)
Hafnium selenide	$HfSe_2$	hcp / CdI_2, Layer	NA
Molybdenum selenide	$MoSe_2$	$HfSe_2$	1150 ± 50
Niobium selenide	$NbSe_2$	$HfSe_2$	< 780
Platinum selenide	$PtSe_2$	$HfSe_2$	NA
Tin selenide	$SnSe_2$	$HfSe_2$	670
Titanium selenide	$TiSe_2$	$HfSe_2$	NA
Tungsten selenide	WSe_2	$HfSe_2$	NA
Zirconium selenide	$ZrSe_2$	$HfSe_2$	NA

Table 2(h) - Potential materials for inorganic water repellents

Category: TELLURIDES

Material Name	Chemical Formula	Crystal Structure	Melting Point (°C)
Cobalt telluride	$CoTe_2$	hcp / CdI_2, Layer	764
Iridium telluride	$IrTe_2$	$CoTe_2$	NA
Nickel telluride	$NiTe_2$	$CoTe_2$	900.5
Palladium telluride	$PdTe_2$	$CoTe_2$	730
Platinum telluride	$PtTe_2$	$CoTe_2$	1150
Rhodium telluride	$RhTe_2$	$CoTe_2$	1075
Silicon telluride	$SiTe_2$	$CoTe_2$	885
Titanium telluride	$TiTe_2$	$CoTe_2$	NA
Zirconium telluride	$ZrTe_2$	$CoTe_2$	1700

Table 2(i) - Potential materials for inorganic water repellents

Category: SULFIDES

Material Name	Chemical Formula	Crystal Structure	Melting Point (°C)
Orpiment	As_2S_3	Monoclinic, Layer	300
Realgar	As_4S_4	Molecular crystal	α-257; β-307
Bismuth sulfide	Bi_2S_3	Double Chain	680
Molybdenite	MoS_2	hcp / CdI_2, Layer	NA
Hafnium sulfide	HfS_2	MoS_2	1185
Platinum sulfide	PtS_2	MoS_2	225 - 250
Stibnite	Sb_2S_3	MoS_2	550
Tin sulfide	SnS_2	MoS_2	600
Tantalum sulfide	TaS_2	MoS_2	> 1300
Titanium sulfide	TiS_2	MoS_2	
Tungsten sulfide	WS_2	MoS_2	1800, d 1250
Zirconium sulfide	ZrS_2	MoS_2	1550

Table 2(j) - Potential materials for inorganic water repellents

Category: NITRIDES

Material Name	Chemical Formula	Crystal Structure	Melting Point (°C)
Boron nitride	BN	hcp, Layer	3000 (subl.*)
Boron nitride	BN	Zinc Blende, 3-D	
Titanium nitride	TiN	Cubic/NaCl	2950
Zirconium nitride	ZrN	Cubic/NaCl	2980
Hafnium nitride	HfN	Cubic/NaCl	3000
Silicon nitride	Si_3N_4	Hexagonal	1900

* subl. = sublimes

Table 2(k) - Potential materials for inorganic water repellents

Category: CARBIDES

Material Name	Chemical Formula	Crystal Structure	Melting Point (°C)
Hafnium carbide	HfC	Cubic / NaCl	3890
Niobium carbide	NbC	HfC	3613
Tantalum carbide	TaC	HfC	3985
Zirconium carbide	ZrC	HfC	3530
Titanium carbide	TiC	HfC	3257
Silicon carbide	SiC	Hexagonal Rhombhohedral Cubic	2540

TABLE 2(l) - Potential materials for inorganic water repellents

Category: BORIDES

Material Name	Chemical Formula	Crystal Structure	Melting Point (°C)
Hafnium diboride	HfB_2	Hex.	3200
Zirconium diboride	ZrB_2	HfB_2	3250
Niobium diboride	NbB_2	HfB_2	3000
Tantalum diboride	TaB_2	HfB_2	3037

Table 3 - Characteristics of some hydrophobic solids

Material	Type of crystal structure	Contact angle [reference]	Flotability [reference]	Cause of break-down with increase in temperature
Diamond	3D		NF*	Oxidation
Graphite	Layer	60 [22]	NF	Oxidation
Boric acid	Layer		NF	Dehydroxyl./PT
Talc	Layer		NF	Dehydroxylation
Pyrophyllite	Layer	82 [t.s*]	NF	Dehydroxylation
Sulfur	Chain	90 [t.s]	NF	Oxidation/PT
Realgar			100 [29]	Oxidation/PT
Stibnite	Double chain	42 [22]	95 [29]	Oxidation/PT
Molybdenite	Layer	80 [26]	100 [29]	Oxidation
Pyrite	3D	135 [27]	100 [29]	Oxidation
Chalcopyrite	3D	131 [27]	75 [29]	Oxidation
Orpiment	Layer		95 [29]	Oxidation/PT
Silver iodide	3D	60 [28]	NF	PT
Boron nitride	Layer	60 [t.s]	NF	Oxidation

* NF= naturally floatable, t.s = this study, PT = phase transformation

IV(a). EXPERIMENTAL INVESTIGATION OF THE HYDROPHOBICITY AND THERMAL STABILITY OF SELECTED MATERIALS [BORON NITRIDE, TALC. AND MOLYBDENITE]

In this section the thermal cycling behavior of three hydrophobic materials, namely boron nitride [BN], talc [$Mg_3(OH)_2(Si_2O_5)_2$] ,and molybdenite [MoS_2] will be discussed. We used these materials as model compounds to study the effect of thermal cycling behavior on their hydrophobicity. The three materials also have melting temperatures that are greater than 800 °C, but they are subject to oxidation or che mical change at higher temperatures. The room temperature water-repellent properties of these materials were known, but their high temperature behavior had not been tested before.

All the materials discussed in this section have a layered structure. Boron nitride has a structure similar to graphite, and the material is electrically neutral within the layers. Between the layers, there are weak van der Waals bonds, that holds the material together.

Talc is a complex oxide material, where each layer consists of two silica tetrahedra sheets sandwiching a magnesium hydroxide octahedral sheet between them (see Figure 2). Each three-layer sheet [SiO/MgOH/SiO] is electrically neutral, with the charge on the two silica tetrahedra in the unit cell being exactly balanced by the charge in the octahedral magnesium hydroxide layer between the two silica layers. Talc crystals are held together by van der Waals forces acting across adjacent SiO/MgOH/SiO sandwich sheets (Figure 2). However, in forming edges on talc crystals, covalent / ionic bonds must be broken, a process that gives rise to reactive highly charged surface sites that readily interact with water molecules. Thus, the wetting behavior of talc is very anisotropic. At high temperature, talc decomposes with the loss of water molecules from the octahedral magnesium hydroxide layer [30].

In molybdenite, each layer consists of two sheets of sulfur sandwiching a sheet of molybdenum atoms (Figure 3). The S/Mo/S layers are held together by van der Waals forces, giving rise to a nonpolar face that is very water repellent. The edges of a molybdenite crystal are formed by breaking MoS ionic bonds, which then gives rise to polar edge sites.

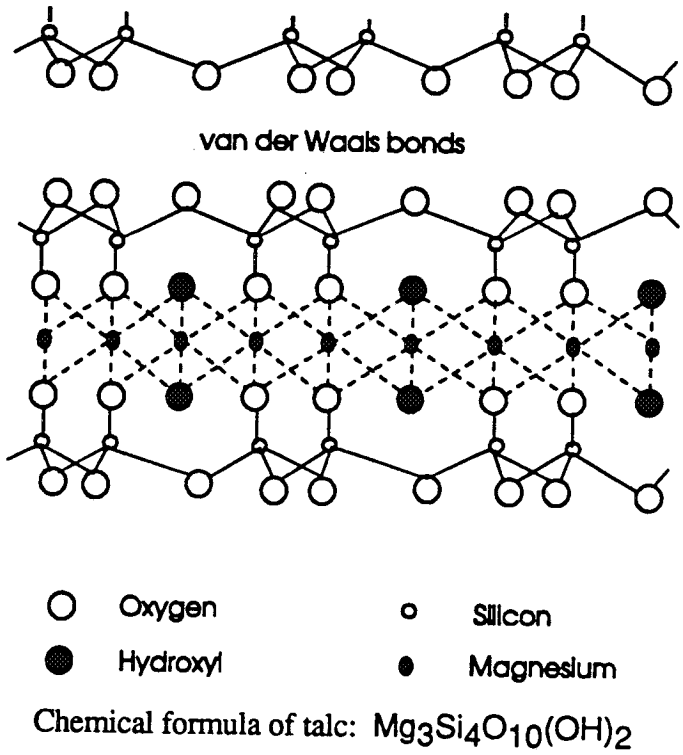

Figure 2- The crystal chemistry and structure of talc (edge view), showing where van der Waals forces act between the SiO/MgOH/SiO layers to form the crystal faces and broken SiO and MgO bonds form the crystal edges.

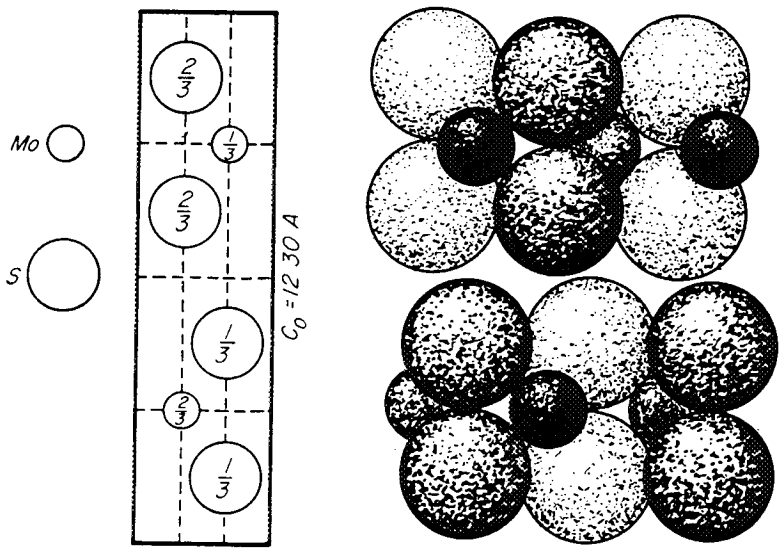

Figure 3- Projection and packing drawing of molybdenite, illustrating the MoS_2 sandwich layers that form the crystal through van der Waals forces acting between them.

Experimental

The samples of BN came from Hermann C. Starck, GMBH & Co., Germany. The talc samples were from Balmat mine in New York, obtained from Wards Natural Science Estab., and the molybdenite samples were from Fortland Arendal (Norway) obtained from Minerals Unlimited.

The starting sample for BN was a fine powder, finer than 1 micron in size. The talc used in these experiments was a 53x75 micron fraction separated by sieving from crushed material. Pellets were made by compacting these powdered samples in a piston-die press. The pellets were used for the thermal cycling experiments, with contact angle measurements being performed by the sessile drop method [15]. Here, a drop of water is placed on the pellet surface (Figure 1) and within the first 15 seconds, the contact angle of the water droplet is measured through a goniometer. For molybdenite, natural pieces were used and since they exhibited a relatively flat surface, the sample did not have to be ground and pelletized. A sulfur pellet, known to exhibit contact angles close to 90 degrees, was used to standardize the sessile drop method for experiments with the other materials.

Two different kinds of experiments were conducted. The first was a thermal cycling experiment in which a pellet formed from the powdered material was heat-treated at various elevated temperatures for a 30-minute duration, after which the pellet was cooled to room temperature. After that heating/cooling procedure, the contact angle of a water droplet was measured using a goniometer. In the second kind of experiment, the number of cycles taken to wet was estimated. Here, for each cycle, the sample was soaked in water at room temperature for one hour, followed by drying at 100 °C for one hour, then cooling the sample to room temperature, following which measurement of the contact angle was then done.

Further characterization of the behavior of boron nitride and talc was carried out by thermal gravimetric analysis (TGA). Here the weight loss or gain of the material was measured as a function of the temperature to which the sample was heated.

Results and Discussion

At temperatures below 800 °C, the contact angle of a water droplet on BN was observed to remain constant at values between 50 to 60 degrees. As the temperature was increased above 800 °C, the contact angle decreased from about 50 degrees to 30 degrees. Surface oxidation is the most likely process for the deterioration of the contact angle on this material. Also, the results of our thermal gravimetric study (TGS), given in Figure 4, showed that a weight gain of BN begins at 900 °C and increases sharply at 1000 °C, indicating the uptake of oxygen and formation of boron oxide (probably B_2O_3). The initial formation of a surface oxide by oxygen adsorption just before bulk oxidation started probably rendered the material hydrophilic.

Talc pellets were found to be completely wetted at 800 °C because of the decomposition of talc, most likely through water the evolution of water formed by dehydroxylation in the octahedral layer of the unit crystal. This was demonstrated by the weight loss that started at 800 °C, as observed by the results of the thermal gravimetric experiments shown in Figure 5. For temperatures up to 600 °C, the measured contact angle of water on the surface of the pellet was 30 degrees. As already stated, talc particles consist of faces and edges. The faces are electrically neutral and contribute to the hydrophobicity of a talc particle. The edges contain broken bonds of silicon-oxygen and magnesium-oxygen. The interaction of water with edge sites contributes to the hydrophilicity. As the particle size of talc decreases, the edge-to-face ratio increases [31], partly because of smearing of the soft material during size reduction, and the talc particles become mostly water wetting. On the same line of argument, coarser talc particles (about 0.2 mm) are more hydrophobic due to the higher ratio of hydrophobic faces to hydrophilic edges. The low magnitude of the contact angles (around 30 degrees), measured here are mostly due to the fine particle size used to form the pellets with their correspondingly higher fraction of edges, as well as random orientation of the particles on the external surface of the pellet.

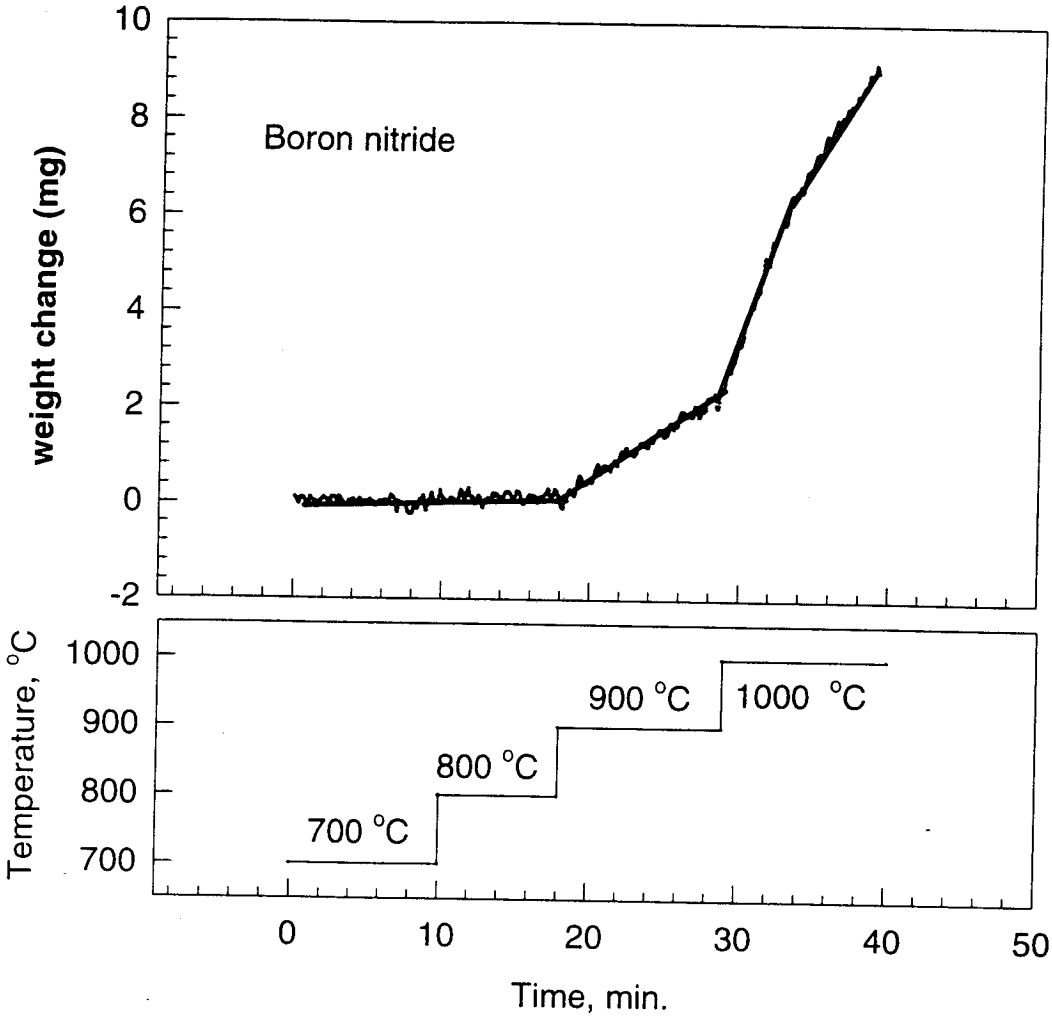

Figure 4- Thermal gravimetric study showing the weight gain of boron nitride as a function of time and temperature. The results show the initiation of boron nitride oxidation at 900 °C and the sharp increase in oxidation at 1000 °C.

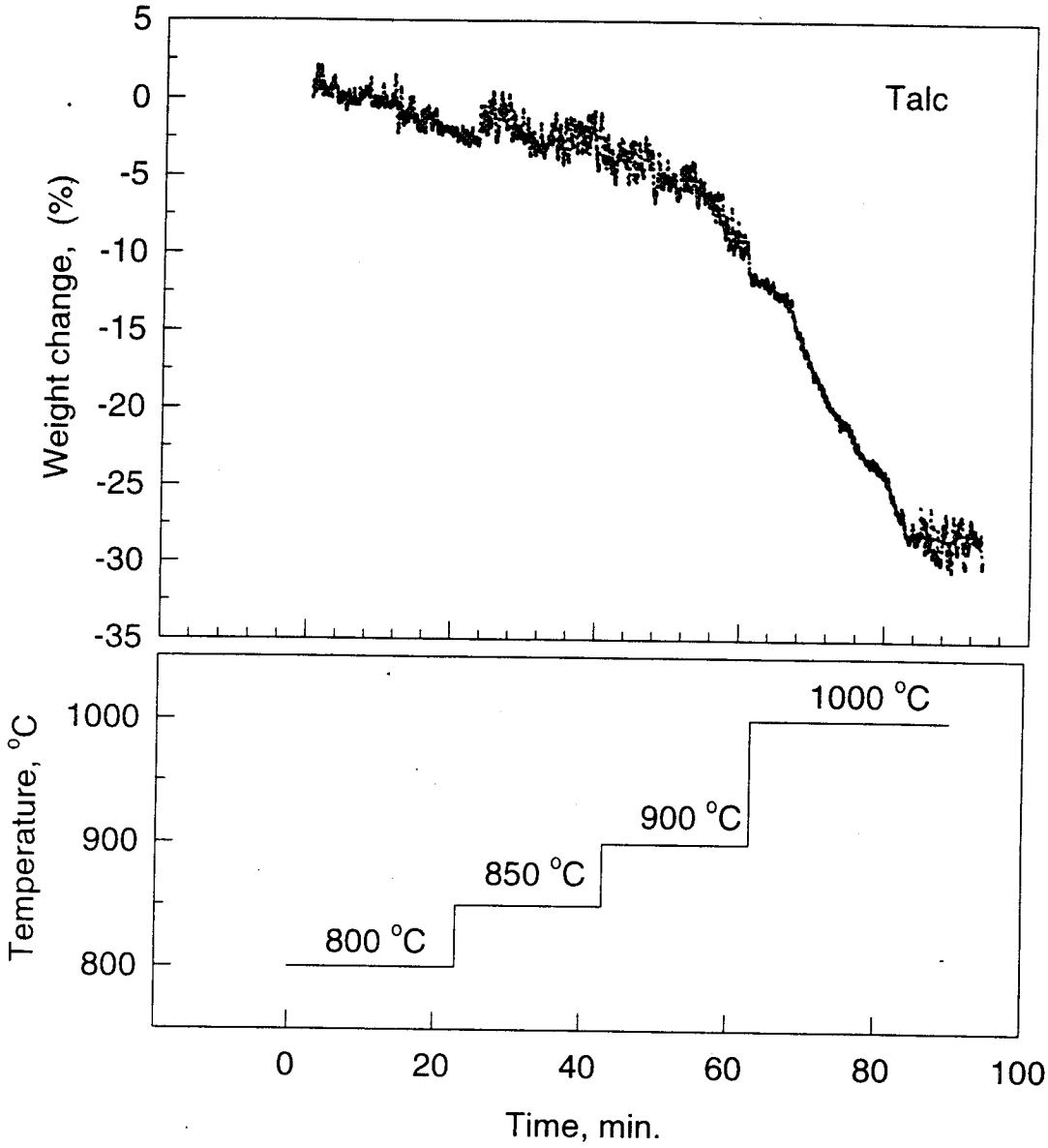

Figure 5- Thermal gravimetric study showing the weight loss of talc as a function of heating time and temperature. The marked weight loss due to the dehydroxylation of talc begins at 800 °C.

A film flotation study was also carried out in order to understand the wettability of coarser talc particles. In this method, aqueous solutions of different surface tensions are prepared (by mixing different amounts of methanol and water) and the amount of material that sinks into and floats on these solutions is estimated by collecting and weighing the respective fractions. The surface tension of the solution corresponding to the 50% float point is used in a model to extract the contact angle values [16]. As estimated from the film flotation results, the contact angle of talc at room temperature is about 65 degrees and decreased to 53 degrees when heated to a temperature of 800 °C, but was only 19 degrees when the temperature was raised above 950 °C. As already stated, the TGA study indicates that the dehydroxylation of talc starts at 800 °C , which clearly indicates that the decrease in the contact angles can be attributed to this process.

In order to minimize oxidation of the samples, the pellets of talc and boron nitride were put into a bag made from a stainless steel sheet material. Argon gas was purged before closing the bag. Before and during the heating cycle, argon was also purged inside the furnace to maintain a positive gas pressure. The samples were then cooled under an argon atmosphere also. All these elaborate procedures were used because a good seal could not be achieved with the stainless steel bags. By taking all these precautions, we hoped that the oxygen concentration in the furnace atmosphere could be substantially reduced. However, our attempts at studying the effect of thermal cycling under an inert argon-purged atmosphere did not yield any significant improvement in the hydrophobicity. That is, the contact angles measured with and without argon gas in the furnace chamber were found to be similar.

Molybdenite is a naturally occurring hydrophobic mineral, but its hydrophobicity decreases with increasing heating temperature due to oxidation. To obtain a fresh surface, specimens of MoS_2 were first washed with triply distilled water and then cleaved. The contact angles were measured on a fresh surface of MoS_2 after thermal cycling at 20, 200, 400 and 600 °C in separate runs. The measured contact angles were 65, 55, 40 and 0 degrees at the respective temperatures. After washing the heated surface with distilled water, the contact

angles were found to increase in general, with the respective contact angles being 65, 60, 60 and 70 degrees. This observed increase in the magnitude of the contact angle on molybdenite had been reported by Chander and Fuerstenau [26] The oxidized product, molybdenum oxide, forms and anionic species in water and thereby dissolves completely in aqueous solution. After removal of the surface oxidation products by dissolution, a fresh surface of molybdenite is now exposed and the contact angle returns to its original room temperature value. However, with further increase in temperature, more of this sulfide mineral will oxidize, limiting its use as a permanent coating material..

The contact angles measured with a water droplet at room temperature on the different materials as a function of thermal cycling are summarized in Table 4.

Table 4- The room temperature contact angles of water (as measured by the sessile drop method) on the surface of the various materials tested as a function of thermal cycling.

Temperature ∞C	20	200	400	600	800	1000
BN (< 1mm)	65	50	50	52	43	35
Talc	20-35	33	30	31	Wetted	Wetted
MoS_2	65	55	40	Wetted		
Sulfur	95					

For the second kind of experiment, the samples were completely soaked in water and later dried and cooled to room temperature for measurement of the contact angle. The boron nitride and talc samples were found to be completly wetted after the first cycle. The cause of the breakdown of water repellency is not completely understood. For molybdenite, the contact angle stayed constant around 50 degrees for the first cycle following which the sample started to lose its hydrophobicity.

A sample of scandium fluoride (a material that had been postulated by NASA Ames as being potentially water-repellent) was submitted by NASA Ames for us to assess its water-repellenc characteristics. This powder was extremely fine and we were unable to prepare the pelletized disk of the material needed for contact angle measurement. Consquently, we were unable to assess the wetting characteristics of this material

Summary

Boron nitride seemed to be water repellent up to temperatures of 800 °C. Above temperatures of 800 °C, BN undergoes surface oxidation which makes the sample hydrophilic. With talc, the breakdown in hydrophobicity coincides with the start of the process of water evolution through dehydroxylation. The different contributions to the overall hydrophobicity of talc is dependent on the edge-to-face ratio of the talc particles. The major breakdown temperature for the water repellency of talc takes place at temperatures greater than 800 °C. In the case of molybdenite, the breakdown of water repellency occurred at 600 °C due to the formation of a hydrophilic surface oxide product. However, when the material is cleaned with water, its hydrophobicity can be restored, as a new molybdenite surface is again exposed.

IV(b). EXPERIMENTAL INVESTIGATION OF THE HYDROPHOBICITY AND THERMAL STABILITY OF PYROPHYLLITE

Pyrophyllite is an aluminosilicate clay mineral that belongs to the category of layered structures with nonpolar faces that are held together by weak van der Waals bonds. It has a sandwich-like structure comprised of three layers, the first and the third corresponds to silica tetrahedra and the second is an interlayer of aluminum hydroxide. Its chemical composition is $Al_2Si_4O_{10}(OH)_4$. Talc is similar to pyrophyllite, differing only by having three magnesium ions subsituting for two aluminum ions in the octahedral layer of the unit cell. Each of the sandwich- like sheets of SiO/AlOH/SiO is electrically neutral. The structure is held together by weak van der Waals forces between these composite sheets. Pyrophyllite is hydrophobic at room temperature and exhibits a contact angle of 80 degrees. In this study, we have tested the use of pyrophyllite as a potential high-temperature water repellent inorganic material.

Pyrophyllite undergoes phase transformation on heating and this has been studied in the literature by two techniques, namely X-ray diffraction and nuclear magnetic resonance (NMR). Pyrophyllite occurs mostly in the triclinic and monoclinic forms. Detailed analysis of the crystal structure of pyrophyllite by X-ray diffraction has been reported by Brindley and Wardle [32]. A summary of the lattice parameters for both the normal and dehydroxylated monoclinic form of pyrophyllite sample (by heating at 800 °C for 96 hours) is listed in Table 5 (from Brindley and Wardle). From an X-ray diffraction study of the triclinic phase of pyrophyllite (the lattice parameters a, b and c are close to the above-mentioned values of the monoclinic phase and the angles α and γ are away from the monoclinic value of 90 degrees by $\pm$ 2 degrees), Wardle and Brindley [33] concluded that the dehydroxylation reaction is homogenous is nature, where pairs of hydroxyl ions react locally to form O^{2-} and water. Also, they predicted that the coordination of aluminum is possibly five-fold in dehydroxylated pyrophyllite. This five-fold coordination has been confirmed by Pedro Sanchez-Soto et al. [34] through a detailed NMR study. These latter authors reported that the silicon atoms occupy

well defined positions in the tetrahedral sheet and the aluminum has a five-fold coordination through the following reaction:

Table 5 - Crystal structure parameters for monoclinic pyrophyllite [32]

	Normal	Dehydroxylated	% expansion
a	5.172 Å	5.173 Å	
b	8.958 Å	9.114 Å	+1.74
c	18.676 Å	18.995 Å	
α	90º	90º	
β	100º	100º	
γ	90º	90º	
d (001)	18.408 Å	18.707 Å	+1.625

$$Al(OH)_2O_4 \rightarrow AlO_5 + H_2O$$

The dehydroxylated pyrophyllite remains crystalline till temperatures below 1000 °C, but between the range of 1000 °C to 1200 °C it is mostly amorphous. Beyond 1200 °C the transformation of amorphous pyrophyllite takes place, resulting in the formation of the new phases, mullite and cristobalite.

Materials and Experimental

The pyrophyllite sample used for all the studies came from Tres Cerritos, Indian Gulch, Mariposa County, California and was obtained from Minerals Unlimited. X-ray diffraction analysis of the sample of pyrophyllite indicated a monoclinic crystal structure. However, in our samples, some of the peaks at 2-theta values around 20 degrees were found to be missing when compared to the data of Brindley and Wardle [32]. Three samples were analyzed. The first corresponds to the "as-is" condition, the second and the third were heat-treated at 600 °C

and 900 °C, respectively, for a 30-minute duration, following which they were cooled to room temperature. We utilized a Siemens D-5000 Diffractometer to characterize the pyrophyllite samples, using Cu-Kα radiation at operating settings of 40 KV and 30 mA. The X-ray diffraction spectrum was indexed with three of its main peaks, corresponding mainly to the (00l) family of reflections. All three samples exhibited very similar spectra, with the only difference coming from the peak heights. To further characterize our sample, we studied the weight loss of a sample of pyrophyllite by thermal gravimetric analysis (TGA). TGA yielded a 4.54% loss in the sample weight starting at 620 °C and being completed at 870 °C. Below temperatures of 620 °C, no weight change was observed.

The water-repellent property of pyrophyllite was first verified for room temperature conditions. The contact angles were measured using the sessile drop technique, where a drop of water is placed on the surface of the material and the contact angle of water is measured with the help of a goniometer. A pellet made from 0.3 x 0.6 mm particles of pyrophyllite exhibits a contact angle between 80 to 90 degrees with water. This high contact angle indicates that pyrophyllite is indeed hydrophobic at room temperature. But, there was no published information on the water repellency of pyrophyllite that had been exposed to higher temperatures. This led to our deciding to investigate the effect of thermal cycling on the wetting behavior of pyrophyllite. In conducting our thermal cycling experiments, a pellet of pyrophyllite was heat-treated at various temperatures for a 30-minute duration after which the pellet was cooled to room temperature in air and then the contact angle of a water droplet was measured on the surface of the pellet. Table 6 summarizes the results obtained from these thermal cycling experiments.

During the thermal cycling experiments, for temperatures greater than 600 °C, noticeable expansion of the sample was observed (primarily through the disintegration of the pellet). These samples were then re-pelletized and the contact angle of a water droplet was measured. The expansion of the samples corresponds very well with the results from Pedro Sanchez-Soto et al. [25] for the linear expansion of pyrophyllite beyond 600 °C (see Figure 6).

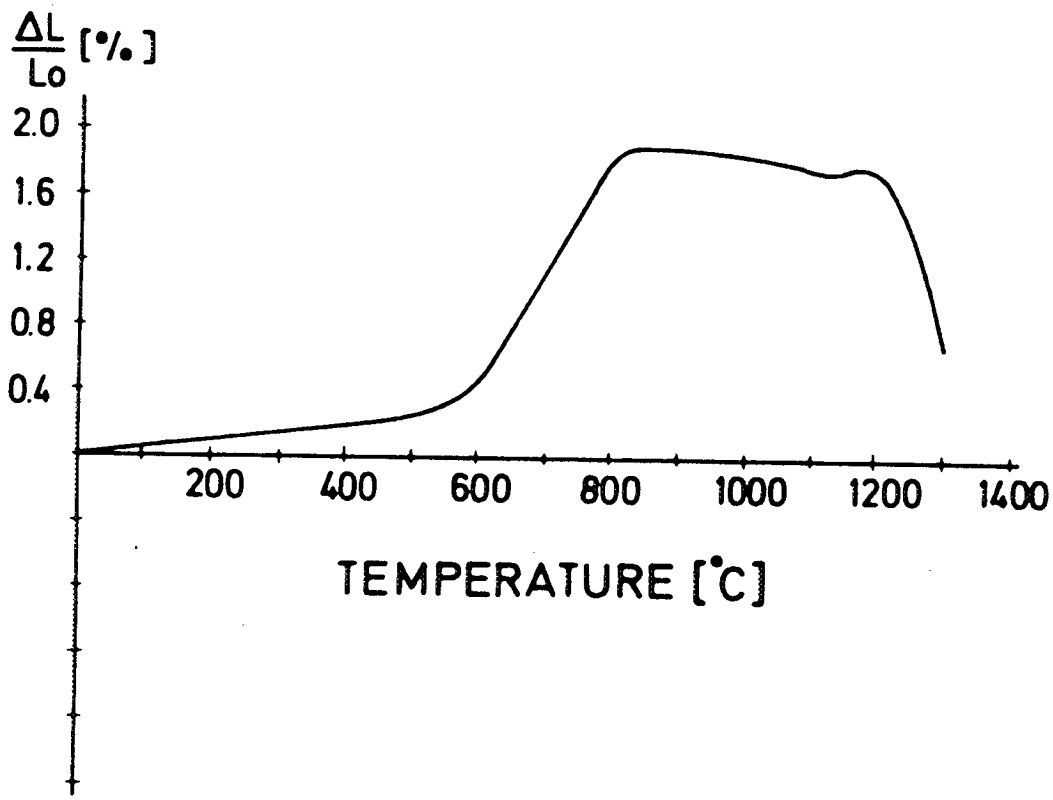

Figure 6- The dilatometric curve showing the thermal expansion of pyrophyllite that begins at 600 °C, which parallels the progressive dehydroxylation of the starting silicate sample. The contraction in the dilatometric curve above 1200 °C is attributed to the formation of the crystalline phases of mullite and cristobalite. The slight contraction above 1000 °C was assigned to decomposition of dehydroxylated pyrophyllite (after Sanchez-Soto et al. [34]).

Table 6 - The contact angle of pyrophyllite measured at room temperature as a function of thermal cycling at various heat-treatment temperatures.

Heat-treatment Temperature, °C	Contact Angle, degrees
200	68
400	68
600	68
800	68
900	65
1000	55
1100	wets

When heated to temperatures between 800 °C and 1000 °C, the predominate phase, dehydroxylated pyrophyllite, shows only a slight decrease in the contact angle of water, compared to the hydroxylated crystal form. Furthermore, when heated to temperatures above 900 °C, eventhough the material was dehydroxylated, pyrophyllite does not wet until it has been heated to a temperature of 1100 °C.

In order to study the effect of dehydroxylation and thermal expansion in detail, the pyrophyllite sample was first soaked at two different temperatures, 600 °C and 900 °C. At 600 °C, the pyrophyllite has neither dehydroxylated nor undergone any expansion. But when heated to a temperature of 900 °C, the sample of pyrophyllite has undergone both dehydroxylation as well as expansion. This heat-treated sample was then cooled to room temperature and a variety of different experiments was carried out with them.

In the first kind of experiment, for each cycle, the pellet was soaked in water at room temperature for one hour, followed by drying it at 100 °C for one hour. After cooling the pellet

to room temperature, the contact angle was measured and the same sample was heated to their respective heat-treatment temperature, either 600 °C or 900 °C. The second kind of experiment involved the measurement of the contact angle of a water droplet on the surface of a pellet as a function of cycling to 600 °C or 900 °C. Here, after the contact angle was measured at room temperature, the same sample was reheated to either 600 °C or 900 °C for a 30-minute soaking period. The last type of experiment involved heating a sample of pyrophyllite to 600 °C or 900 °C and then that material was formed into pellets that were heat-treated to various temperatures so that the effect thermal cycling at the different temperatures could be investigated.

Results

The results obtained from the various kinds of experiments on the effects of temperature cycling are summarized below in the tables that follow.

For this first series of experiments, the pyrophyllite pellet was soaked in water at room temperature for one hour, followed by drying it at 100 °C for one hour, and after cooling the sample to room temperature, the contact angle was measured. The results from three such cycles are given in Table 7.

Table 7 - Study of room-temperature wet-dry cycling on the contact angle of pyrophyllite.

Cycle Number	Contact Angle, degrees
1	83
2	67
3	50

In the next series of experiments, for each cycle the pyrophyllite pellet was first heated to 600 °C for 30 minutes, followed by cooling it to room temperature after which the pellet was

soaked in water at room temperature for one hour. After drying it at 100 °C for one hour and cooling it to room temperature, the contact angle was measured by the sessile drop method. The results are tabulated in Table 8. A second set of experiments was carried out identical to the foregoing except that the pellet was heated to 900 °C, and those results are given in Table 9.

Table 8 - Study of room-temperature wet-dry cycling on the contact angle of pyrophyllite that had been heated to 600 °C.

Cycle Number	Contact Angle, degrees
1	68
2	52
3	33

Table 9 - Study of room-temperature wet-dry cycling on the contact angle of pyrophyllite that had been heated to 900 °C.

Cycle Number	Contact Angle, degrees
1	50
2	48
3	37

As part of our studies on the effect of high temperature cycling, the room temperature contact angles of a water droplet on the surface of a pyrophyllite pellet were measured as a function of thermal cycling to 600 °C. For each cycle, the same sample was reheated to 600 °C for a 30- minute soaking period. The results of these tests are given in Table 10. To ascertain the behavior of pyrophyllite cycled to higher temperatures, a series of experiments was carried

out similar to those given in Table 10, except that the pellet was heated to 900 °C in each cycle. The results of these experiments are tabulated in Table 11.

Table 10 - Study of the thermal cycling behavior of pyrophyllite between room temperature and 600 °C on its contact angle.

Cycle Number	Contact Angle, degrees
0 (start)	70
1	70
2	60
3	58
4	40

Table 11 - Study of the thermal cycling behavior of pyrophyllitebetween room temperature and 900 °C on its contact angle.

Cycle Number	Contact Angle, degrees
0 (start)	60
1	50
2	48
3	37
4	wets

In this series of experiments, the powdered pyrophyllite was first heated to 600 °C and then that material was formed into pellets which were heat-treated at various temperatures, ranging from 200 °C to 1100 °C. In each case, the pellets were cooled to room temperature after heat-treatment for contact angle measurements. The results are summarized in Table 12.

Table 12. Study of the thermal cycling on the contact angle of pellets prepared from pyrophyllite that had first been preheat-treated at 600°C.

Heat-Treatment Temperature, °C	Contact Angle, degrees
20	70
200	70
400	68
600	68
800	67
900	67
1000	47
1100	wets

Table 13. Study of the thermal cycling on the contact angle of pellets made from pyrophyllite that had been preheat-treated at 900°C.

Heat-Treatment Temperature, °C	Contact Angle, degrees
20	68
200	65
400	61
600	62
800	57
900	54
1000	36
1100	wets

Discussion

Pyrophyllite appears to have good water-repellent properties after being heated to temperatures up to 900 °C. Under these conditions, the sample has undergone complete dehydroxylation, but still retains a crystalline structural order. In the first kind of experiments that were carried out, the wet-dry cycling behavior of pyrophyllite was investigated. As can be seen from the results of these experiments given in Tables 7 to 9, the pyrophyllite sample exhibited consistent behavior for the three tested temperatures, that is room temperature, 600 °C and 900 °C. In all these cases, there is only a slight drop in the contact angle of water for the first two cycles. These experiments were designed to prove that even when the sample is completely soaked in water, its water-repellent properties do not deteriorate substantially. For conditions where the sample sees only small quantities of water, such as in the form of water droplets, a second kind of experiments was performed, the results of which are reported in Tables 10 and 11. As could be observed from the results of the first kind of experiments, the contact angle of water decreases by a small amount over the first two cycles, beyond which the sample ultimately wets out after a total of four cycles. The amount of water does not seem to play a major role in the deterioration of the water-repellent properties of pyrophyllite. The decrease in the contact angle of water could result from possible cracking occurring from the repeated expansion and contraction of the pellets during the thermal cycling process, which may have led to the formation of submicron size pores. It is important to remember that in this study, we have used cold-pressed pellets. Possibly, hot-sintering the pellets may improve the number of cycles to which a pyrophyllite sample would preserve its water-repellent behavior.

In the last kind of experiment, after first heating the material to either 600 °C or 900 °C, a pyrophyllite pellet was prepared by cold pressing and that pellet was heat-treated at various temperatures ranging up to 1100 °C. Without this initial heating to 600 °C and to 900 °C, starting from room temperature, the pyrophyllite sample showed only a very small variation between 65 and 70 degrees for the contact angles of water (Table 6). Initial preheating the

pyrophyllite to 600°C before making the pellet that was subsquently cycled to various temperatures produced a material that gave very similar values for the contact angles of water, when compared with the sample that had been produced from room temperature material (Tables 12 and 13). However, initial preheating of the pyrophyllite powder to 900 °C produced pellets whose contact angles after heat-treatment at the respective temperatures were lower than those given for non-heat-treated starting material (Table 6). The drastic drop in the contact angle beyond 1000 °C can be attributed to the breakdown of the structure through the formation of the amorphous phase. Once, the pyrophyllite sample has expanded completely by initally preheating it to a temperature of 900 °C, on subsequent heating there is very little visible change in the shape of the pellets. Therefore, for the use of pyrophyllite as a water repellent material where exposures to high temperatures may be involved, pretreating at 900 °C could prevent the sample from undergoing any future thermal expansion.

Scanning electron microscopy (SEM) was used to study the microstructure of the heat-treated pyrophyllite samples. At room temperature, the pyrophyllite samples exhibited flat faces with sub micron size fragments clinging on to them and edges that are like a stack of sheets (like playing cards) stuck together. With increase in the temperature to 600 °C, there is no apparent change in the microstructure of the faces, but most of the changes start taking place along the edges. The edges begin to delaminate and at 900 °C the distance between the delaminated sheets (like a deck of cards) increases. This would then correspond to the sample expansion that was observed at temperatures higher than 600 °C.

Conclusions

Pyrophyllite is a good water repellent material that is capable of preserving its hydrophobicity even when heated to temperatures around 900 °C. From the wet-dry cycling experiments and the thermal cycling to either 600 °C or 900 °C, it can be concluded that for the first two cycles changing the amount of water in contact with a pyrophyllite pellet, either

through immersion or in the form of a droplet, had little effect on the contact angle. The deterioration of the contact angle upon further cycling may be attributed to the microscopic cracking resulting from repeated expansion and contractions. As a design strategy, when used as a water-repellent material at high temperatures, it might be best to pre-process the pyrophyllite starting material at 900 °C and then conform it to the required shape to prevent any expansion problems. Dehydroxylated pyrophyllite retains its crystallinity even at 900 °C and a certain amount of water repellency, but beyond 1000 °C it completely loses its water repellency due to the breakdown of its layer structure.

V. MODELING HYDROPHOBICITY OF SOLIDS HAVING THREE-DIMENSIONAL COVALENT/IONIC BONDS

In this section we would like to introduce a new parameter based on the fractional ionic character in the chemical bond and combining it with the hard-soft acid-base principle to predict the hydrophobicity of inorganic compounds. The classification of the whole range of materials can be done into elements, molecular crystals, layered materials and three-dimensional materials. Bonding in these materials is either metallic, covalent, ionic or van der Waals. Hydrophobicity of a material has been the most important variable for studying their floatability (that is, their attachment to air bubbles). Most hydrophobic solids exhibit some extent of natural floatability, and the non-floatable solids can be made floatable through the adsorption of heteropolar molecules/ions that have specific functional polar groups and a nonpolar hydrocarbon chain (as exemplified by typical surfactants) [35]. Previous studies on predicting the natural hydro-phobicity of materials have started from the viewpoint of crystal structure. Gaudin et al. [20] viewed natural floatability as the lack of breakage of primary interatomic bonds present on a cleavage or fracture surface of a material. In their work, they have stated that "*the natural lack of floatability results when all natural fracture or cleavage surfaces offer bonds to the surrounding liquor than some threshold value.*" Any material that is nonpolar and is held together by weak van der Waals bonds along the plane where fracture takes place is likely to be hydrophobic. This description works well in most cases, but cannot be used to explain the hydrophobicity observed in some three-dimensional structures, such as silver iodide, diamond, and others, where the fractured surface exposes broken bonds.

Hydrophobicity of a material arises due to its noninteraction with water molecules. When water molecules wet a surface, we can define this through the energy associated with the work of adhesion. As given in Section II, the work of adhesion of water with a solid surface can be written as:

$$W_A = W_A^d + W_A^h + W_A^{el} \tag{19}$$

The first term is the contribution from the van der Waal (dispersion) interactions; the second term is the hydration term which comes from the hydrogen bonding interaction of water with the surface hydroxyl sites; and the last term is the electrical term which estimates the contribution from the ionic sites on the solid surface. Fowkes and others [11, 18] have modified the work of adhesion to include all types of acid-base interactions, W_A^{AB}, given by the following expression:

$$W_A = W_A^d + W_A^{AB} + W_A^{el} \qquad (20)$$

Usually a solid is hydrophobic when the contribution from the last two components are small and the dispersion energy is the main term. The work of adhesion term related to the dispersion forces (van der Waals term) is the most important term for making a solid hydrophobic. Laskowski and Kitchener [17] showed that this term is always less than the work of cohesion of water, and concluded that "*all solids would be hydrophobic if they did not carry polar or ionic groups.*"

In the following section, we would like to revisit the partial ionic character of various bonds in molecules as proposed by Pauling [36] and try to apply this methodology in combination witht the hard-soft acid-base principle for correlating the observed hydrophobicity of various materials.

Covalent-Ionic Character in a Bond

For the molecule A-B, the partial nature of the ionicity of the bond could be considered as a mixture of the extremes, completely ionic and completely covalent. In the case of ionic AB, the bonding is as A^+-B^- and for covalent A:B. In the first case, the electron density is located more towards the B atom, and the second case involves the sharing of the electron, giving rise to a directional bond.

For the molecule A-B, the difference in the energies between an arithmetic mean or a geometric mean of the individual A-A and B-B bonds with an A-B bond gives an estimate of

the extent of ionic or covalent nature in them. The fraction of ionicity of the bond depends on the relative electronegativities of the atoms in consideration. Pauling [36] defined electronegativity as *"the measure of the tendency of an atom in a molecule to attract electrons to itself."* Pauling summarized the extra ionic energy between A-B as the following:

$$\Delta'(A\text{-}B) = 30\ (x_A\text{-}x_B)^2 \qquad [24]$$

where x_i represents the electronegativity of atom i. The bond energy is then estimated as

$$E(A\text{-}B) = 0.5\ [\ E(A\text{-}A) + E(B\text{-}B)]\ +\ 23\ (x_A\text{-}x_B)^2 \qquad [25]$$

where E represents the bond energies [$30\ (x_A\text{-}x_B)^2$ instead of $23\ (x_A\text{-}x_B)^2$ would appear in Eq. 25 if the expression were in terms of a geometric average]. The heats of formation of molecules could be estimated from the above expression (except for cases where double and triple bonds are formed).

Pauling [36] used the concepts of electronegativities and proposed a relation (empirically obtained by fitting a whole range of simple molecules) for the amount of ionic character, $\%I_p$, in a chemical bond:

$$\%I_p\ =\ 100\ [1 - \exp\ (-0.25\ (x_A\text{-}x_B)^2\ )] \qquad [26]$$

The above expression works well over the range of simple compounds tested and the improvements that have been proposed use the means (arithmetic and geometric) of the electronegativity values, but leaves the functional form of the expression intact [37]. Equation 26 provides a means for obtaining a qualitative estimate of the amount of ionic character in different types of compounds.

Hard-Soft Acid-Base principle (HSAB)

The concept of hard-soft acid-base principle has to be used in conjuction with our estimation of the fractional ionicities in various bonds. According to the original definition, a

Lewis acid is an electron pair acceptor and a Lewis base is an electron pair donor [38]. In modern terminology, a Lewis base is any substance that has electron density that can be shared with another substance in a chemical reaction and a Lewis acid is any substance capable of accepting electron density.

Lewis acids and bases can be classified on a scale of hard to soft [39]. Soft bases (or ligands) are large molecules that are easily polarized, that is they readily donate electrons to form covalent bonds. Soft bases selectively bond with soft acids, typically metal ions of relatively large radius and low charge. Hard bases tend to be small molecules that are not easily polarized and tend to form less covalent bonds and more ionic bonds, typically with metal ions of small radius and high charge. Cations that fall into the hard-acid category include the IA group, IIA group, Al (III), Fe (III), Ti (IV), Zr (IV), Si (IV), Cr (VI) and more. Some of the anions that fall into the hard-base category are OH^-, O^{2-}, F^-, Cl^-, H_2O, NH_3, perchlorate, sulfate, phosphate, nitrate, carbonate, and acetate. Cations belonging to the soft-acid category are Cu (I), Ag (I), Hg (I), Hg (II), Cd (II), Pt (II), Pt (IV), Pd (II), Au (I) and Tl (I). Some anions that fall into the soft-base category are CN^-, I^-, thiosulfate, and thiocyanate. There are some cations and anions that belong to the intermediate type of acids or bases, respectively. These ions can act as either hard or soft depending on the chemical interaction with their respective acid or base counterpart.

Most transition metal oxides are more stable with respect to their corresponding other bases. This is because, in oxides, the interaction is of the hard acid - hard base type. In addition, the enthalpies of formation reported in the literature support this assertion. Similarly amongst the soft acid - soft base compounds, their corresponding oxides have a lower stability.

Pauling's formula for estimating the fractional ionic character in various bonds has been used to estimate in the following classes of compounds: sulfides, oxides, halides, selenides, tellurides, nitrides and carbides. The values obtained are tabulated for the various classes of materials in the tables that follow. The heat of formation for the various bonds have been reported, as they correspond directly to the stability of the compound and its suscepti-

biility to oxidation. Also, for some of the compounds (selenides and tellurides), their decomposition temperatures have been included, since very little is known about their water-repellent properties.

Table 14(a) - Ionic character estimated in metal-sulfur bonds

M-S	$\|\Delta p\|$	$\%\|p$	ΔH_f, 298 K (x,y) kcal mole^{-1}
W	0.22	1.2	25 (1,2)
Pb	0.25	1.6	24 (1,1)
Pt	0.30	2.2	12.67 (1,2)
As	0.40	3.9	13.47 (2,3)
Mo	0.42	4.3	28.1 (1,2)
Sb	0.53	6.8	13.93 (2,3)
Bi	0.56	7.5	11.4 (2,3)
Hg	0.58	8.1	13.9 (1,1)
Ag	0.65	10	7.79 (2,1)
Ni	0.67	11	19.6 (1,1)
Cu	0.68	11	12.7 (1,1)
Fe	0.75	13	21.3 (1,2)
Cd	0.89	18	38.7 (1,1)
Zn	0.93	19	49.23 (1,1)
Zr	1.25	32	67.65 (1,2)
Na	1.65	49	87.2 (1,2)

ΔH_f is the enthalpy of formation per gram-atom of S at 298 K in kcal mole^{-1}. These data are taken from Reference 23.

In the fourth column, (x,y) represents M_xS_y stoichiometry.

In the second column, the quantity $|\Delta p|$ is the difference in the electronegativities for each of the kind of bonds considered (sulfides in this case). The data are taken from Reference 36.

In the third column, the amount of ionic character $\%|p$ given by Eq. 26.

Table 14(b) - Ionic character estimated in metal-oxygen bonds

M-O	$\|\Delta p\|$	$\%I_p$	ΔH_f, 298 K (x,y) kcal mole^{-1}
Pb	1.11	27	51.47 (1,1)
Pt	1.16	29	9.75 (3,4)
As	1.26	33	44.2 (2,5)
Mo	1.28	34	59.4 (1,3)
Sb	1.39	38	57.4 (2,3)
Hg	1.44	40	21.4 (1,1)
Ag	1.51	43	7.42 (2,1)
Ni	1.53	44	57.3 (1,1)
Si	1.54	45	108.9 (1,2)
Cu	1.54	45	37.1 (1,1)
Zn	1.79	55	83.24 (1,1)
Al	1.83	57	133.5 (2,3)
Zr	2.11	67	130.8 (1,2)
Na	2.51	79	99 (2,1)

ΔH_f is the enthalpy of formation per gram-atom of O at 298 K in kcal mole^{-1}, and (x,y) represents M_xO_y stoichiometry

Table 14(c) - Ionic character estimated in silver-halide bonds

Ag-X	$\|\Delta p\|$	$\%\|p$	ΔH_f, 298 K (x,y) kcal mole^{-1}
F	2.05	65	48.9 (1,1)
Cl	1.23	32	30.37 (1,1)
Br	1.03	23	23.99 (1,1)
I	0.73	12	14.78 (1,1)

ΔH_f is the enthalpy of formation per gram-atom of X at 298 K in kcal mole^{-1}, and (x,y) represents Ag_xX_y stoichiometry

Table 14(d) - Ionic character estimated in metal-selenide bonds

M-Se	$\|\Delta p\|$	$\%\|p$	ΔH_f, 298 K (x,y) kcal mole^{-1}	Decomposition Temperature, °C
Pb	0.22	1.20	24.6 (1,1)	1065
Pd	0.35	3.02	*NA (1,2)	1000
Bi	0.53	6.78	NA (2,3)	710
Ga	0.74	12.79	NA (2,3)	1020
In	0.77	13.78	NA (2,3)	890
Cd	0.86	16.88	NA (1,1)	1350
Zn	0.90	18.33	NA (1,1)	1100

ΔH_f is the enthalpy of formation per gram-atom of Se at 298 K in kcal mole^{-1} and (x,y) represents M_xSe_y stoichiometry.

Decomposition temperatures are obtained from Reference 24.

*NA: data not available

Table 14(e) - Ionic character estimated in metal-telluride bonds

M-Te	$\|\Delta p\|$	%Ip	ΔH_f, 298 K (x,y) kcal mole^{-1}	Decomposition Temperature, °C
Bi	0.08	0.2	6.17 (2,3)	573
Pt	0.18	0.8	NA (1,2)	1200
Pb	0.23	1.3	NA (1,1)	917
Ga	0.29	2.1	NA (1,1)	824
In	0.32	2.5	NA (1,1)	696
Cd	0.41	4.1	22.1 (1,1)	1121
Au	0.44	4.7	NA (1,2)	472
Zn	0.45	4.9	NA (1,1)	1238

ΔH_f is the enthalpy of formation per gram-atom of Te at 298 K in kcal mole^{-1} and (x,y) represents M_xTe_y stoichiometry.

Table 14(f) - Ionic character estimated in metal-nitride bonds

M-N	$\|\Delta p\|$	%I_p	ΔH_f, 298 K (x,y) kcal mole^{-1}
B	1.0	22	60.8 (1,1)
Si	1.14	28	44 (3,4)
Ti	1.5	43	80.4 (1,1)
Zr	1.71	52	87.3 (1,1)

ΔH_f, Enthalpy of formation per gram-atom of N at 298 K in kcal mole^{-1}
(x,y) represents M_xN_y stoichiometry

Table 14(g) - Ionic character estimated in metal-carbide bonds

M-C	$\|\Delta p\|$	$\%\|p$	ΔH_f, 298 K (x,y) kcal mole^{-1}
Si	0.65	10	16 (1,1)
Ti	1.01	23	44.1 (1,1)
Zr	1.22	31	47 (1,1)

ΔH_f, Enthalpy of formation per gram-atom of C at 298 K in kcal mole^{-1}
(x,y) represents M_xC_y stoichiometry

Table 14(h) - Ionic character estimated in metal-fluoride bonds

M-F	$\|\Delta p\|$	$\%\|p$	ΔH_f, 298 K (x,y) kcal mole^{-1}
Sc	2.62	82	NA (1,3)
Zr	2.65	83	114.2 (1,4)
Y	2.78	86	136.93 (1,3)

ΔH_f, Enthalpy of formation per gram-atom of F at 298 K in kcal mole^{-1}
(x,y) represents M_xF_y stoichiometry

Discussion

Compounds that may be hydrophobic can be classified based on two aspects. First, the fractional ionic character of the bond is estimated. Compounds that are predominantly covalent in nature, possessing a fractional ionicity of less than 20 percent (an arbitrary choice)tend to be hydrophobic. For the second aspect, it would be necessary to classify which hard-soft acid-base category that the ions constituting the bond belong to. The ions to be considered are those which are present on a fractured surface (it is necessary to satisfy the first aspect as well). Our hypothesis is that if either of the ions is of the hard acid or hard base type, then the resulting surface would be hydrophilic. If either of the ions belong to the soft type, then most likely the solid surface would tend to be hydrophobic. If, however, it is of the mixed type, then it is a "may be" hydrophobic situation, and would be hydrophobic if the intermediate type ions do not bind or combine strongly with either H^+or OH^- or O^{2-}.

From Table 14(a), it is clear that most sulfides which are predominantly hydrophobic have fractional ionicity values less than 20 percent, and that the cations belong to the soft-acid category. Let us then postulate that any material whose calculated fractional ionicity has a value less than 20 percent will tend to be hydrophobic. For some of the complex sulfides, say chalcopyrite, $CuFeS_2$, the value of ionic character could be taken as an average of both Cu-S and Fe-S, namely 13 percent.

Most of the oxides have fractional ionicity value more than 20 percent [see Table 14(b)] and they belong to the hydrophilic category. An O-H bond has a fractional ionicity value of 40 percent. The hydrophilic nature of most oxides is mostly due to the extensive hydrogen bonding that takes place at the surface between surface hydroxyls and water molecules.

It is interesting to see the trend predicted for the silver-halides, particularly in relation to the known hydrophobicity of silver iodide [28]. Because of this nature, silver iodide is widely employed for cloud seeding. The calculated Pauling ionicity of silver iodide is 12 percent, whereas the rest of the silver halides have values greater than 20% [Table 14(c)] . In fact, silver fluoride is an ionic compound that dissolves completely in water; both silver chloride and

silver bromide are sparingly soluble; and silver iodide has the lowest solubility product of all the silver-halides. Both silver and iodide belong to the soft acid-base category.

As reported in Tables 14(d) and 14(e), most of the metal selenide and telluride bonds are covalent in nature and, according to our hypothesis, should be hydrophobic in nature. Some of the compounds listed have fairly high decomposition temperatures and complete data for the enthalpies of formation are not even known. It is possible that some metal selenides and tellurides may have the required high-temperature water-repellent property.

Amongst the nitrides, the hexagonal form of boron nitride is known to be a hydrophobic material [20]. Boron nitride has a graphite-like hexagonal structure, where the layers are held together by weak van der Waals bonds. It also has a fractional ionicity value of 22 percent. We measured the contact angle of water on the surface of two forms of boron nitride at room temperature, the first was a pellet formed from hexagonal boron nitride powder (as reported in Section IVa), and the other was an amorphous thin film of boron nitride on a quartz substrate. In both these cases, we measured contact angles of very similar magnitude, 60 degrees, with a water droplet.

For the carbides, silicon carbide may exhibit hydrophobicity if we view the solid as being predominantly covalent in nature. But one of the ions that belonging to the fractured surface is Si (IV), which is a member of the strong-acid category. Therefore, even with its predominantly covalent nature, silicon carbide might be expected to be hydrophilic. Also, in the presence of moisture or oxygen atmosphere and at increased temperatures, silicon carbide forms a silica surface layer, rendering itself hydrophilic.

In terms of this concept, fluorides would be expected to be hydrophilic. This is partly due to the fact that fluorine is the most electronegative element in the Periodic Table and is also a strong base. Since the fractional ionicity is calculated based on a difference in the electro-negativities of the elements involved in the formation of their bond chemical bond, the estimated values indicate predominantly ionic bonds.

There are some drawbacks in using fractional ionicity values for predicting the hydrophobicity of materials. Some problems are related to the manner in which electronegativity values were proposed by Pauling: the theoretical basis for the electronegativity scale and the dependence on the atoms bonding environment in its compounds (oxidation state, coordination number, hybridization and others) [41]. Other problems come from the way ionicity is defined, that is, as a quantity depending on the difference in the electronegativity of the atoms. Therefore, if both the atoms involved in forming the bond are similar, the model would predict 100 percent covalent nature. Also, this model is difficult to extend to organic compounds, a large fraction of which are hydrophobic. As mentioned earlier, in some complex sulfides like chalcopyrite, we could possibly estimate an average ionicity based on its individual members. This however may not work for all cases. Therefore, we should have to limit this method to analyze simple inorganic compounds.

As mentioned previously in Section II, water molecules can interact with ionic surface sites on the solid, by hydrogen bonding with surface oxygen and surface hydroxyls, and by dispersion forces. In the case of nonpolar solids, the main interaction term is only that of the dispersion term, a phenomenon that renders the solid hydrophobic because of the very great tendency of water to hydrogen bond with itself. The three different interactions are responsible for the ordering of water next to various surfaces. Parry and Evans [42] have suggested that the water molecules undergo a phase transformation and exist as a gas phase next to nonpolar surfaces. Also, within only a couple of molecular layers, the properties of bulk water are achieved. On the basis of our assumed limit of 20 percent on the fractional ionicity, and if the ions belong to the category of soft acid-base type, we then assume that the solid surface should be mostly nonpolar and hence exhibit water repellency. However, hydrophobicity is a complex function of the crystal chemistry, the nature of chemical bonding, the kind of surface functional groups that are exposed, contamination on the surface, the nature of the chemical environment in which the solid is present, surface charge characteristics in solution, the degree of surface roughness, microporosity on the external surface of the particle and thermal cycling

sequence at higher temperatures. By using our ionicity calculation as a first step, looking at the category to which the ions consituting the surface (broken bonds) belong, and later collecting the relevant details from the crystal structure, and finally asking the question about the orientation of water next such a solid interface should help provide an approach to fully understanding the natural hydrophobicity of inorganic solids.

With respect to design of other inorganic materials for space vehicle application, based on our model the metal of choice could be from the soft-acid category, where the tendency to bond with a strong base like oxygen is minimized. Some of the materials that fall into this category containing the bonds: Pt-Te, Au-Te and Pd-Se, where these compounds have higher melting temperatures than their corresponding oxides (these compounds, like the sulfides, may be susceptible to oxidation).

Conclusion

The Pauling electronegativity values have been used to estimate the fractional ionic character in broken bonds for various types of compounds. Our hypothesis is that compounds that have fractional ionicities less than 20% and those whose constituent ions are of the soft acid-base category should have a higher probability of being hydrophobic. Most of the sulfides, selenides, tellurides fall in this category. In the case of oxides, however, the fractional ionicity is greater than 20 percent and the oxygen anion belongs to the hard-base category, causing them to be hydrophilic.

VI. SUMMARY OF THE REPORT

Most naturally occurring hydrophobic materials have layered structures that are held together by weak van der Waals bonds between them. In order to identify potential inorganic water-repellent materials, a list of compounds (mostly having a layered structure) was first compiled. A "candidate" material was one that would exhibit water-repellency even after being heated at elevated temperatures (600 °C), and retain its hydrophobicity after repeated thermal cycling. Typical factors that would lead to the breakdown of water-repellency of materials are phase transformation; oxidation; and chemical decomposition (for example, dehydroxylation). Therefore, by considering the physical and material properties, a few candidate materials that would retain their hydrophobicity at elevated temperatures were selected. The materials tested could be considered hydrophobic for nonporous surfaces but none of the observed contact angles exceeded the necessary 90 degrees required for water repellency of porous materials.

The materials that were tested as "candidate" materials included boron nitride, molybdenite, talc, and pyrophyllite. Boron nitride seemed to be water repellent up to temperatures of 800 °C. Above temperatures of 800 °C, BN undergoes surface oxidation which causes the material to become hydrophilic. In the case of molybdenite, the breakdown of water repellency occurred at 600 °C due to oxidation, which resulted in the formation of a hydrophilic surface oxide product. However, when the molybdenite was cleaned with water, its hydrophobicity was restored, as a new molybdenite surface is again exposed because the oxidation product is the water-soluble molybdate ion. Oxidation is the main contributor to the deterioration of water-repellency for both boron nitride and molybdenite.

Both talc and pyrophyllite are layered complex oxides of silicon, where each layer consists of two silica tetrahedra sheets that sandwich between them a magnesium hydroxide octahedral sheet in the case of talc and aluminum hydroxide in the case of pyrophyllite. The SiO/MgOH/SiO triple layers, which are electrically neutral, are held together in the crystal by weak van der Waals forces. With talc, particle size seems to play a role in determining the

onset of loss of hydrophobicity. Coarser particles (about 0.2 mm in size), which have a greater ratio of neutral face to polar edge surface, were observed to retain their hydrophobicity when heated to temperatures below 800 °C, at which temperature the dehydroxylation of talc begins. However, finer particles which have a lower percentage of faces as compared to polar edges were found to be water-wetting in nature. Pyrophyllite appeared to have significant promise in terms of retaining its water-repellency after being heated to temperatures around 900 °C and its withstanding up to two rounds of thermal cycling. There was a small change in the contact angle of a water droplet from 70 degrees to 65 degrees after heating in the temperature range from 200 °C up to 900 °C. Also, for wet-dry thermal cycling, the contact angle of a water droplet ranged between 70 degrees at the beginning to 48 degrees at the end of two cycles. In order to actually use pyrophyllite as an high-temperature water-repellent material, due to its expansion, it would be necessary to first heat the sample to temperatures between 600 °C and 900 °C.

To understand the hydrophobicity of materials, a model using the physical properties of the elements was developed. The model assumes that the hydrophobicity is related to both the extent of ionicity of the bonds and the polarizable nature of the ions involved in forming the bond. Pauling's electronegativity values for atoms represent the starting point in this estimate of the fractional ionic character in a bond between two elements. Assuming that compounds that have fractional ionicity values less than an arbitrary value of 20 percent are considered to be predominantly covalent in nature. Not all materials that are in this category would be expected to be hydrophobic. The second necessary condition is that the elements which are involved in the bonding are easily polarizable, that is, the respective constituent ions belong to the soft acid-base category. When both the conditions are met, then those compounds should have a greater probability of being hydrophobic. Since most oxides exhibit fractional ionicities greater than 20 percent and with the oxygen anion belonging to the hard base category, oxides are predominantly hydrophilic. However, most of the sulfides, iodides, selenides, and tellurides have fractional ionicities less than 20 percent, which, when combined with a soft

cation, leads to these compounds being hydrophobic. Silver iodide is one such example. The proposed soft acid-base / ionicity model appears to offer an interesting approach for screening inorganic materials for their hydrophobic/hydrophilic characteristics.

VII. REFERENCES

1. "Decision Criteria for the Reusable Launch Vehicle Technology Program Phase II and III," Comments Developed by OMB/Energy and Science, OSTP and NASA.

2. H. S. Greenberge and T. Tu, "Test Plans, Lightweight Durable TPS: Tasks 1, 2, 4, 5 and 6," NASA - CR - 196867.

3. P. M. Sawko and H. E.Goldstein, "Performance of Uncoated AFRSI Blankets During Multiple Space Shuttle Flights," NASA-TM-103892, RECON 92N29104.

4. C. Schomburg, R. L. Dotts, and D. J.Tillian, "Moisture Adsorption Characteristics of the Orbited Thermal Protection System and Methods Used to Prevent Water Ingestion," Intersociety Conference on Environmental Systems, July 11 -15, 1983, Lyndon B. Johnson Space Center.

5. H. W. Wyholds, "A Survey of Waterproofing Procedures for Shuttle," NASA Contract Report, April 21, 1994.

6. C. S. Marvel, "Thermally Stable Polymers", Proceedings of the Conference on Polymeric Materials for Unusual Service Conditions, Moffet Field, CA, Marcel Dekker, (1972).

7. P. E. Cassidy, Thermally Stable Polymers: Synthesis and Properties, Robert A. Welch Foundation, N. Y., Marcel Dekker, (1980).

8. Advanced Surface Coatings: A Handbook of Surface Engineering, D. S. Rickerby, and A. Matthews, Eds., Chapman and Hall, New York (1991).

9. S. Chander, J. M. Wie, and D. W. Fuerstenau, "On the Native Floatability and Surface Properties of Naturally Hydrophobic Solids," AIChE Symposium Series, Vol. 71, No. 150, pp. 183-188 (1975).

10. A.W. Adamson, Physical Chemistry of Surfaces, 5th ed., John Wiley & Sons, New York (1990), 777 pp.

11. Wettability, J. C. Berg., Ed., Marcel Dekker, New York (1993), 531 pp.

12. Contact Angle, Wettability and Adhesion, K.L. Mittal, Ed., VSP, Utrecht, The Netherlands (1993), 971 pp.

13. Wetting, SCI Monograph No 25, London (1967), 448 pp.

14. Modern Approaches to Wettability: Theory and Applications, M.E. Schrader and G.I. Loeb, Eds., Plenum Press, New York, (1992) 451 pp.

15 A. W. Neumann and R. J. Good, Techniques of Measuring Contact Angles, in Surface and Colloid Sci. Vol. II, R. G. Good and R.R. Stromberg, Eds., Plenum Press, NY, pp. 31-91 (1973).

16. D. W. Fuerstenau, J. Diao and J. S. Hanson, "Estimation of the Distribution of Surface Sites and Contact Angles on Coal Particles from Film Flotation Data," Energy & Fuels, Vol .4, 34-37 (1990).

17. J. S. Laskowski and J. A. Kitchener, "The Hydrophilic-Hydrophobic Transition on Silica," J. Colloid & Interface Science, Vol. 29, pp.670-679 (1967).

18. Acid-Base Interaction: Relevance to Adhesion Science and Technology, K. L. Mittal and H. R. Anderson , Eds., VSR, Zeist, The Netherlands, 388 PP. (1991).

19. F.M. Fowkes, "Attractive Forces at Interfaces," I&EC, Vol. 56, p.4 (1964).

20. A. M. Gaudin, H L Miaw and H R Spedden, "Native Floatability and Crystal Structure," in Proceedings, 2nd Congress of Surface Activity, pp. 202-219 (1957).

21. D. W. Fuerstenau, S. Chander and J. M. Wei, "On the Native Floatability and Surface Properties of Naturally Hydrophobic Solids," AIChE Symposium Series, Vol. 71, No. 150, pp. 183-188(1975).

22. N. Arbiter, Y. Fujii, B. Hansen and A. Raja, " Surface Properties of Hydrophobic Solids," AIChE Symposium Series, Vol. 71, No.150, pp. 176-182 (1975).

23. "Physical Constants of Inorganic Compounds," CRC Handbook of Chemistry and Physics D. R. Lide, Ed., CRC Press Inc., pp.4-41 to 4-119 (1991).

24. Handbook of Refractory Compounds, G. V. Samsonov and I. M. Vinitskii, Eds., IFI / Plenum Press, New York, pp. 37-169 (1980).

25. M.C. Fuerstenau and B. J. Sabacky, "On the Natural Floatability of Sulfides," Int. Journal of Mineral Processing, Vol. 8, pp. 79-84 (1981).

26. S. Chander and D.W. Fuerstenau, "On the Natural Floatability of Molybdenite," Trans. A.I.M.E., Vol. 252, pp. 62-69 (1972).

27. V.A. Glembotskii,V. I. Klassen and I.N. Plaksin, Flotation, Primary Sources, New York, Ch. 2, pp. 13-27 (1963).

28. D. W. Fuerstenau and O. Gutsche, "On the Natural Hydrophobicity and Flotability of Silver Iodide," to be published.

29. N. P. Finkelstein, S. A. Allison, V. M. Lovell and B. V. Stewart, "Natural and Induced Hydrophobicity in Sulfide Mineral Systems," in Advances in Interfacial Phenomena, P. Somasundaran and R. B.Grieves, Eds., AIChE. Series 150, Vol. 71, pp. 165-175 (1975).

30. L. J. Michot, F. Villiesas, M Francois, J. Yoon, R. LeDred and J.W. Cases, "The Structural Microscopic Hydrophilicity of Talc," Langmuir, Vol. 10, pp. 3765-3773 (1994).

31. P. Huang, "Interfacial Phenomena in the Flotation of Talc," M.S. Thesis, University of California at Berkeley, (1994), 65 pp.

32. G.W. Brindley and R. Wardle, "Monoclinic and Triclinic Forms of Pyrophyllite and Pyrophyllite Anhydride," Amer. Mineralogist, Vol. 55, pp. 1259-1272 (1970).

33. R. Wardle and G.W. Brindley, "The Structure of Pyrophyllite, 1Tc, and of its Dehydroxylation," Amer. Mineralogist, Vol. 57, pp. 732-750 (1972).

34. P. J. Sanchez-Soto, I. Sobrados, J. Sanz and J. L. Perez-Rodriguez, "29-Si and 27-Al Magic-angle Nuclear Magnetic Resonance Study of the Thermal Transformation of Pyrophyllite," J. Amer. Ceramic Soc., Vol. 76, pp.3024-3028 (1993).

35. A.M. Gaudin, Flotation, Mc Graw-Hill, New York, (1957), 573 pp.

36. L. Pauling, The Nature of the Chemical Bond, Cornell University Press, Ithaca, (1960) 450 pp.

37. A.H. Nethorcot Jr., "Molecular Dipole Moments and Electronegativity," Chem. Phys. Letters, Vol. 59, pp. 346-350 (1970).

38. R. Drago and N.A. Matwiyoff, Acids and Bases, D. C. Heath and Company, Boston (1968)

39. M.B. McBride, Environmental Chemistry of Soils, Oxford University Press, New York, p. 17 (1994).

40. M. Yekeler, S. Aksu, and B. Yarar, "Model for the Prediction of the Critical Surface Tension of Wetting of Low Surface Energy Minerals", in Processing of Hydrophobic Minerals and Fine Coal, pp. 17-27 (1996)

41. M. C. Day Jr. and J. Seblin, Theoretical Inorganic Chemistry, Reinhold Book Corp., New York, pp. 73-155 (1969).

42. A. O. Parry and R. Evans, "Influence of Wetting on Phase Equilibria: A Novel Mechanism for Critical-Point Shifts in Films," Phys. Rev. Letters., Vol. 64, pp. 439-442 (1990).

44. A. F. Wells, Structural Inorganic Chemistry, Oxford Press, Oxford (1962), 1055 pp.